ANL-5849
Reactors - Power
(TID-4500, 14th Ed.)
AEC Research and
Development Report

ARGONNE NATIONAL LABORATORY
P. O. Box 299
Lemont, Illinois

DYNAMIC BEHAVIOR OF BOILING REACTORS

by

J. A. Thie

May, 1959

Operated by The University of Chicago
under
Contract W-31-109-eng-38

DISCLAIMER

TABLE OF CONTENTS

DYNAMIC BEHAVIOR OF BOILING REACTORS

J. A. Thie

ABSTRACT

Eight boiling reactors, BORAX I, II, III, IV, EBWR, LITR, VBWR, and SPERT I have been operated to date, and a considerable amount of information exists in regard to their tendencies toward self-induced power oscillations. Data is presented on the following characteristics of the oscillations: power, pressure, temperature, reactivity amplitudes and their rate of change; thresholds, and harmonic content. Results from three techniques of measuring the reactor transfer function are presented: the rod oscillation, the reactivity step, and the autocorrelation methods. Quantitative definitions of instability are introduced.

Theoretical analysis of these reactors' kinetic behavior, based on a simple model where steam void feedbacks dominate, shows an adequate understanding of many of the phenomena, some even quantitatively. It is concluded that it is possible within the framework of existing experimental and theoretical boiling reactor dynamic technology, to design these reactors with reduced instability limitations on the power, and obtain power densities in excess of the current 50 kilowatts/litre of core.

I. INTRODUCTION

In the field of boiling reactor technology one of the current problems is the limitation imposed on the maximum power by unstable oscillations. In addition to being a challenging scientific problem it is one whose solution will be of great practical benefit, for a reactor's economics is strongly dependent on its power capabilities. Furthermore the theories and experiments dealing with boiling reactor instability will no doubt have analogous applications in stability analyses of other reactor types.

The current status of instability experiments is that they are quite extensive rather than intensive. This is the result of a variety of boiling reactors being operated, and stability information being byproducts of a variety of simple experiments. This wide range of experience is summarized here. It should be useful in testing out current theories and in providing a guide for future experiments of the intensive type.

To define what is meant by instability it is necessary to classify the reactor power, as a function of time, into three categories:

1) Stable operation in which the rms amplitude of the "boiling noise" (i.e., random power fluctuations about the mean) is greater than that of any single frequency, but less than the mean value of the power.

2) Small oscillatory operation in which a periodic power fluctuation exceeds the noise, but whose peak to peak amplitude is less than twice the mean power.

3) Unstable operation having peak to peak power fluctuation in excess of twice the mean power.

The last category is variously referred to as "chugging," or "divergent oscillations." The latter is misleading since all oscillations in nature are initially divergent as they build up from zero amplitude, but are eventually convergent because non-linearities and losses eventually limit the amplitude. This oscillating behavior is an old problem, originating in 1952,[1,2] but only recently has been publicized.[3,4]

Table I

PRESSURE AND POWER RATINGS OF BOILING REACTORS OPERATED TO DATE

Reactor	Maximum pressure in psig	Maximum power in megawatts
LITR[1,2]	0	1.8
BORAX I[5,6]	130	1.2
BORAX II[7]	300	8
BORAX III[7,8]	300	15
BORAX IV[9,10]	300	20
SPERT I[3]	0	6
EBWR[11,12]	620	60
VBWR[13]	1000	30

Table I lists the boiling reactors for which information is currently available. Appendices A, B, and C give basic engineering and physics information about the five Argonne reactors. In this connection it should be pointed out that these experimental reactors were operated under a variety of conditions and configurations, all of which could not be summarized.

II. CHARACTER OF OSCILLATIONS

A. Amplitude Envelope

When a system breaks into oscillation it makes a transition from an amplitude of zero to some final amplitude. In the case of boiling reactors, the initial part of this transition is difficult to observe because of the boiling noise. However, investigation of the rate of increase of the amplitudes is readily possible when they exceed the boiling noise.

The peak powers in a series of "diverging" chugs are not simply related to one another, but it is expected that the reactivity be of the form.

$$k \sim \exp(-\zeta \omega t) \sin \omega t \tag{1}$$

where ζ is the damping constant of the system, and the angular frequency, $\omega = 2\pi f$. To determine ζ for the example shown in Fig. 1, the reactor kinetics equations were solved (AVIDAC code Re-31) for the reactivity when given this power, and the amplitudes of the successive reactivity oscillations plotted to give Fig. 2. In this example the reactor was scrammed, rather than allowing further buildup. Other examples not requiring a scram, are found to have a constant ζ for the first several oscillations. But when the amplitude becomes constant at its maximum value, ζ becomes zero.

An approximate method of obtained Fig. 2 directly from Fig. 1 is to use the relation,

$$\text{Reactivity amplitude} = \left(\frac{\frac{P_i + P_{i+2}}{2} - P_{i+1}}{\frac{P_i + P_{i+2}}{2} + P_{i+1}} \right) \div G_0 \tag{2}$$

where P_i, P_{i+1} and P_{i+2} are the three peaks in one cycle and $G_0 = \left(\frac{p/P^0}{k} \right)_0$ is the zero power reactor transfer function. Since this technique tends to eliminate even harmonics in a frequency range where G_0 is slowly varying for typical cases, reactivity amplitudes almost as large as a dollar are accurate to within a few cents.

In Fig. 3 ζ is obtained for a SPERT I instability (namely, Fig. 6 in Ref. 3). The points are shown to demonstrate an effect also found in analyses of several BORAX II chugging tests: the envelope of the reactivity amplitudes varies cyclically about a pure exponential, with a period several times that of the chugs.

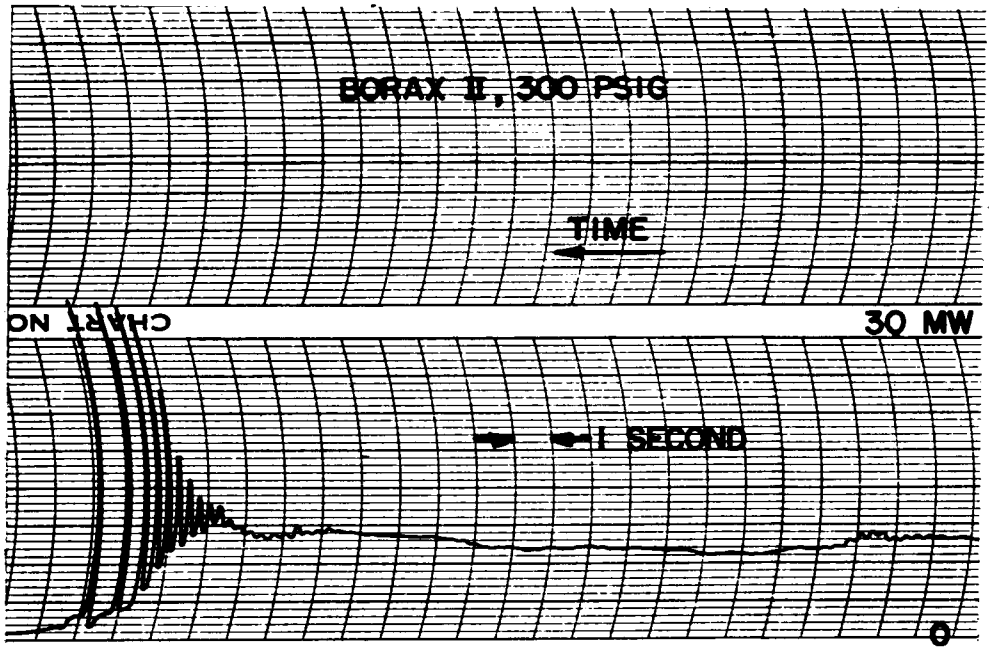

Fig. 1 Transition from Small Oscillatory to Unstable Operation of BORAX II with 72 Fuel Elements and 4% Reactivity in Voids.

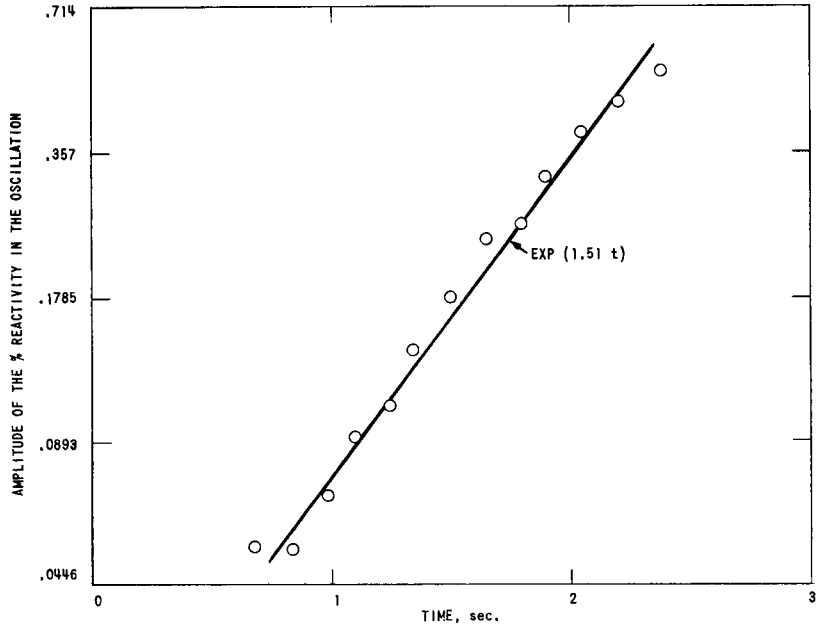

Fig. 2 Reactivity Amplitudes of the Divergent Oscillations shown in Fig. 1.

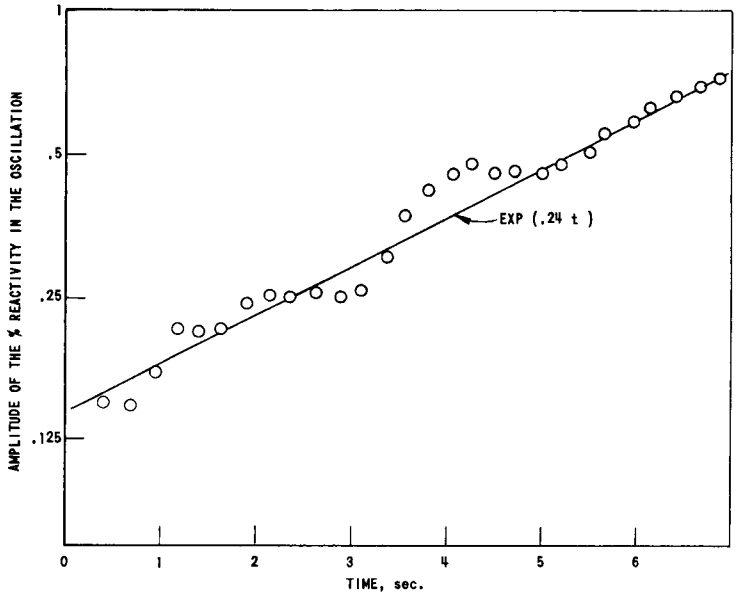

Fig. 3

Reactivity Amplitudes of Divergent SPERT I Oscillations.

Table II summarizes these and other results. Although ζ does not vary too widely among the cases treated, it should be noted that buildups in which $|\zeta|$ is small probably are not observable in presence of boiling noise. The one trend that is worth noting is that $|\zeta|$ increases as the reactivity in voids increases.

Table II

DAMPING CONSTANTS OF REACTIVITY FOR DIVERGENT OSCILLATIONS

Reactor	Pressure in psig	Power in MW	% Reactivity in voids	Frequency in cps	Initial Value of ζ
SPERT I	0	6	(<2.5%)	2.13	-.0180
BORAX II (43-12)*	150	3.8	2.8	2.56	-.0174
BORAX II (46-12)	150	4	2.8	2.84	-.0247
BORAX II (46-12)	150	4	2.8	2.79	-.0160
BORAX II (46-12)	193	4.9	3.4	3.57	-.0326
BORAX II (69- 3)	309	9.5	4.0	3.54	-.0149
BORAX II (69- 3)	300	10.1	4.2	3.54	-.0680

*This notation refers to 43 "lights" and 12 "heavies." See Appendix A.

When a reactor is in the stable region there is of course no envelope to the oscillations and the above technique of damping constant evaluation is not applicable. However a fairly simple experimental determination is possible by use of the so-called "ringing" experiment of Section III-C.

B. Amplitude

When a reactor is in the state of small oscillatory operation defined in Section I, two types of behavior have been observed: that at the beginning of Fig. 1, and that of Fig. 4. The latter is a rare type of oscillation and is distinguished from the former by two characteristics:

a) The cyclic component, p, of the power, while much less than the average power, P^0, nevertheless far exceeds any noisy component.

b) Even though $p/P^0 << 1$ a substantial content of higher harmonics can occur in the waveform of p.

No attempt will be made here to understand this type of oscillation in Fig. 4, for it was only observed in EBWR at low pressures. However, it is speculated that the reactor acted as a "water density meter" during a purely hydraulic instability.

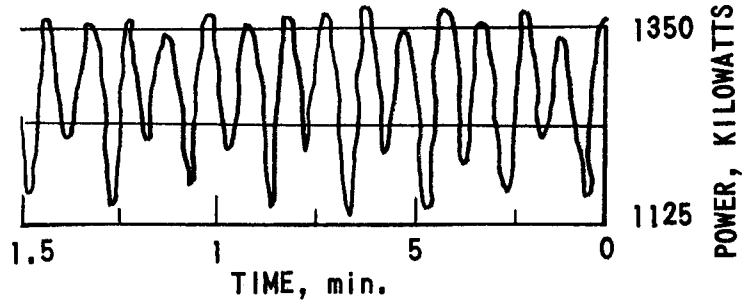

Fig. 4

EBWR Power Oscillations at Atmospheric Pressure, (from Table V and Fig. 14 of Reference 12).

Fig. 5 shows the power dependence of p/P^0 for both this rare type and the ordinary type of oscillation in EBWR. In the case of the latter, a precise oscillatory amplitude is difficult to obtain because of the noise. The procedure used however is to average the larger amplitudes found in many small oscillatory bursts. (The extreme right of Fig. 1 is an example of a small oscillatory burst.)

A more significant feature of ordinary boiling reactor oscillations is that the fraction of voids that oscillate increases with reactor power. The ordinate of Fig. 6 is obtained by dividing the oscillatory reactivity, $(p/P^0) \div G_0$, by the total measured reactivity in voids.

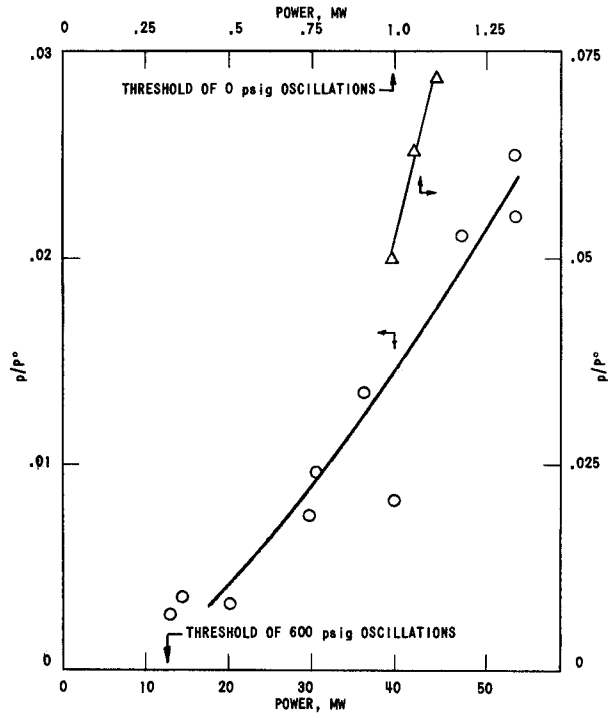

Fig. 5

Power Dependence of the Amplitude of the two Types of EBWR Oscillations

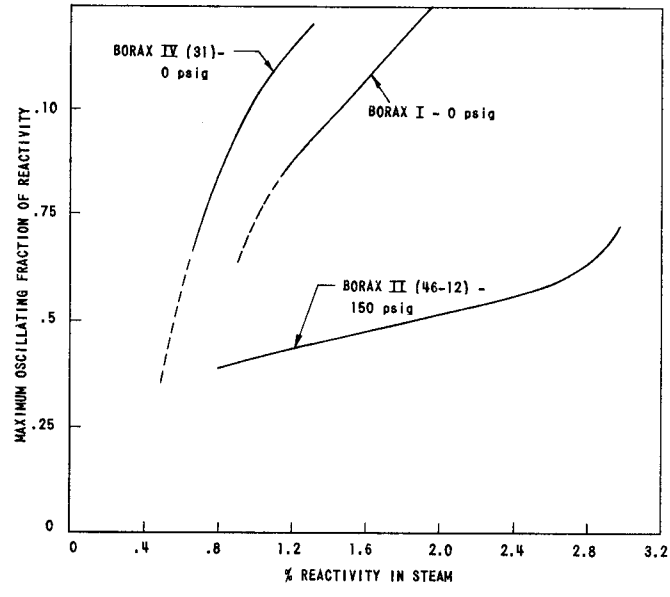

Fig. 6

Maximum Oscillatory Fraction in Voids as a Function of the Reactivity in Voids

The study of a quantity like reactor stability is hampered when no generally quantitative measure of it is accepted. From what has been presented so far it is obvious that merely assigning "yes" or "no" values in ones' personal nebulous concept of stability is not only not quantitative, but leads to disagreement among observers. Unlike electronic oscillators (which either oscillate or fail to oscillate), reactors have a continuous transition from extremely stable to extremely unstable conditions. The following are measures of this continuum:

1. P_ζ, the probability per second of an oscillatory envelope being damped by a constant less than ζ.

2. P_R, the probability per second of the power exceeding R times the average power.

3. The rms value of the power fluctuations.

4. The half-width of the power spectrum. (Section III-D)

5. The reactor transfer function, particularly the height and half-width of any resonance.

While the first definition is a well suited criterion of reactor safety it is somewhat laborious to obtain P_ζ in practice. However some information can be had by determining the largest spontaneous ζ, (as in Table II) or obtaining ζ from ringing tests, (as in Section III-B).

An example of a well-studied case is the EBWR at 45.6 MW and 600 psig:

Table III

MEASURES OF EBWR STABILITY

ζ from ringing tests:	+.13
P_R for R = 1.0364	.34 sec^{-1}
Rms value of p, i.e. $\sqrt{\overline{p^2}}$ (includes noise as well as the dominant oscillatory frequency):	.83 MW
Half-width of the resonance in the power spectrum from autocorrelation techniques:	.18 cps
Properties of the transfer function, G,	
Value at resonance:	55.4 decibels
Half-width of resonance:	.38 cps

Figure 7 is a histogram of this reactor's power fluctuations, p. It is seen that these have a Gaussian distribution.

C. Frequency

Table IV and Fig. 8 show a variety of frequencies are encountered. It might be noted that, as one expects, the lower frequencies occur for reactors of larger size and/or longer fuel element time constant (see Appendix A and Table VIII). Figure 8 (and also Fig. 11) shows an example of frequency increasing as the reactor power level is gradually increased,

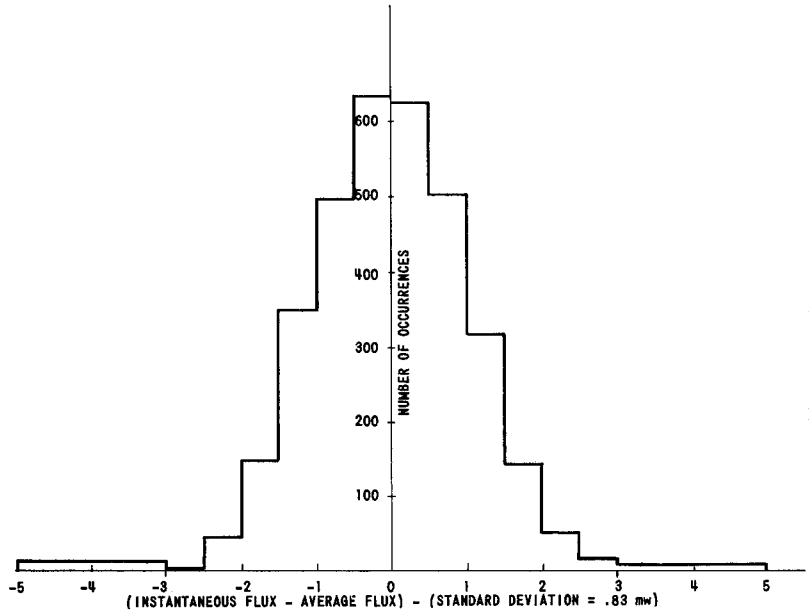

Fig. 7

Histogram of 3331 Consecutive EBWR Fluxes .05 Seconds Apart During 45.6 MW Operation.

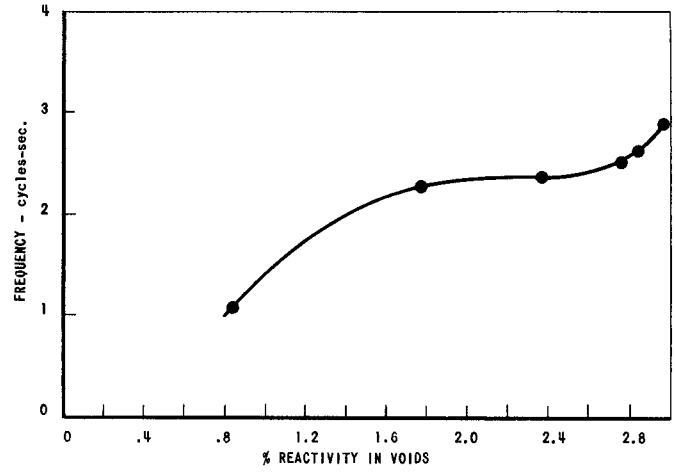

Fig. 8

Oscillation Frequency of BORAX II (46-12) at 150 psig

Table IV

FREQUENCIES OF REACTOR OSCILLATIONS ENCOUNTERED

Reactor	Frequency in cps
BORAX I	1.25
BORAX II	1.0 to 3.3
BORAX III	2.8
BORAX IV	.5 to 2
EBWR (low pressure)	.05, .09, .15, and .28
EBWR (high pressure)	.8 to 1.7

while maintaining small oscillatory conditions. When very violent oscillations exist, as at the end of Fig. 1, the frequency markedly is reduced. This is presumably due to the additional time required for the water to move large distances without benefit of proportionately large velocities.

D. Temperature

As the power oscillates, the fuel temperatures are expected to oscillate, and Table V shows the transfer functions from self-oscillatory conditions of several reactors. Amplitudes of surface, θ_{sur}, or center, θ_{cen}, temperature fluctuations are divided by p/P^0 to obtain the amplitude of this transfer function. The negative phases indicate the temperatures lag the powers.

Table V

FUEL TEMPERATURE TRANSFER FUNCTIONS OF THE BORAX REACTORS

	BORAX I	BORAX II	BORAX IV
Pressure in psig	0	190	0
Frequency in cps	1.25	2.22	.495
$\lim_{p/P^0 \to 0} [\theta_{sur}/(p/P^0)]$ in °F		12.75 $\angle$-32°	
$[\theta_{sur}/(p/P^0)]_{p/P^0 = .5}$ in °F	$-\angle$-13.5°	6.25 $\angle$-32°	5.64 $\angle$-44.6°
$[\theta_{cen}/(p/P^0)]_{p/P^0 = .5}$ in °F	$-\angle$-13.5	—	10.22 $\angle$-141.2°

E. Steam Dome Pressure

Because of insensitive pressure transducers used in BORAX, only violent self-oscillatory reactor conditions could be used in measuring steam pressure oscillation amplitudes. The transfer function obtained by dividing the recorded pressure amplitude by the power amplitude, p, therefore depends on the latter in Fig. 9.

A single observation in BORAX III at 14.5 MW and 300 psig was made for $p/P^0 = .09$. The 2.8 cps swing of a televised pressure gauge needle per unit power fluctuation was .07 psi/MW.

On the other hand an extremely sensitive pressure sensing system used for the EBWR steam dome gave a transfer function of .0263 psi per MW at 600 psig 50 MW conditions. Pressure and small spontaneous power oscillations were exactly out of phase.

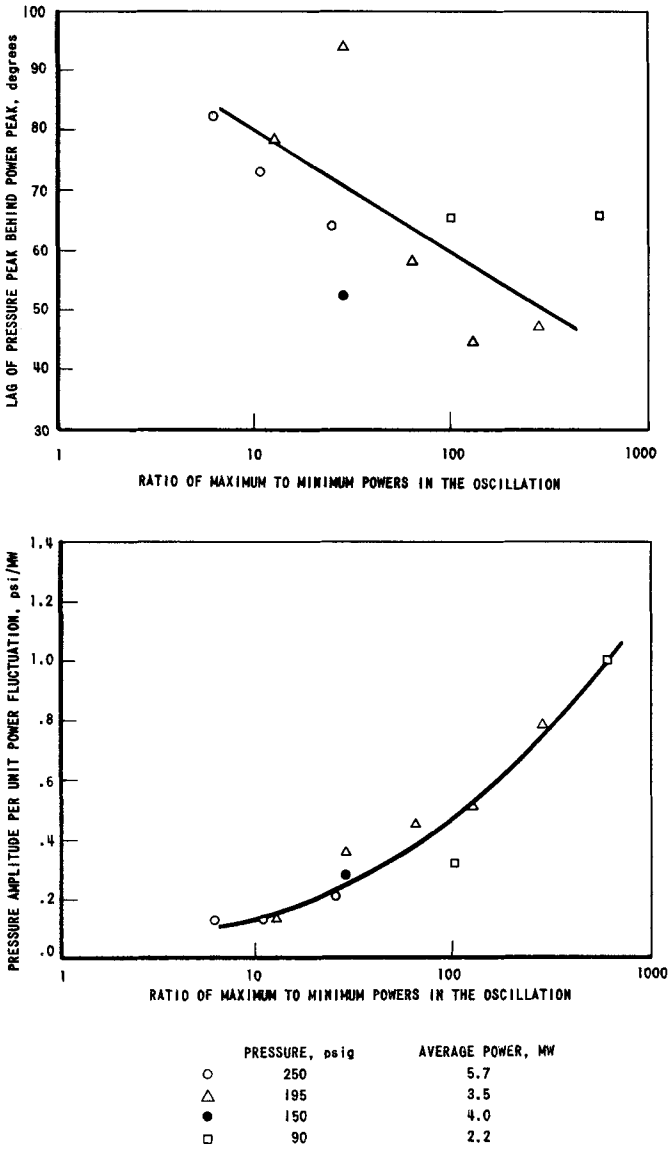

Fig. 9 Power Amplitude Dependence of the BORAX II Steam Pressure Transfer Function

F. Threshold

One definition of the oscillatory threshold is that set of reactor conditions at which the transition from stable operation to small oscillatory operation occurs. To more sharply define this, the method used here requires two or more self-induced cycles (of the same period) in succession without noticeable phase shifting by boiling noise. The data of Table VI gives the correct trends for the power threshold. It must be pointed out

that pressure, fuel element time constant, void coefficient, water channel geometry, and water height above the core are some of the factors affecting this threshold.

Table VI

SMALL OSCILLATION THRESHOLDS

Reactor	Pressure in psig	% Reactivity in voids	kw/litre of core
BORAX I	0	<1.4	<6.14
BORAX II	150	1.2 ± .4	7.9 ± 2.6
BORAX II	300	3.2	21.0
BORAX IV	0	.4	8.41
BORAX IV	100	4.0	14.7
EBWR	0	<.4	.586
EBWR	600	1.3	7.86

In simple systems an oscillatory threshold may be synonymous with an infinite transfer function. However in boiling reactors, (as is seen later in Fig. 20 and 21) comparatively broad and low resonances in the transfer function are had at and even beyond the threshold as defined above. It is theorized that the boiling noise is sufficiently "shaped" by the reactor to exhibit small oscillatory conditions in a mathematically stable system.

G. Harmonic Content

In the data from small oscillatory operation of boiling reactors to date basically two types of waveforms have been observed:

Type A: essentially sinusoidal with very low harmonic content. In this category the amplitudes generally have a randomly shaped envelope, and the oscillatory signal to noise ratio is usually relatively low.

Type B: non-sinusoidal, sometimes with a very high harmonic content. Here the amplitudes tend to have a reasonably constant value, and a high cyclic signal to noise ratio is had.

The small oscillatory part of Fig. 1 is an example of the first, while Fig. 4 is an example of the second. For type A the reactivity waves are virtually pure sine waves, while for type B these have essentially the same harmonic structure as the power oscillation. Because of these differences it might be supposed that two different mechanisms of generating self-sustained reactor oscillations exist. These are discussed in Section IV.

When type A oscillations lead to unstable operation, as in Fig. 1, their amplitudes became highly non-sinusoidal. Numerical solution of the neutron kinetics equations for such cases, however, invariably shows virtually sinusoidal reactivity oscillations. The formulae of Appendix D are used in Table VII to test the postulate of sinusoidal reactivity accompanying a highly non-sinusoidal power oscillation. It can be seen that the harmonic structure is well understood.

Table VII

HARMONIC CONTENT OF A NON-SINUSOIDAL TYPE A POWER OSCILLATION IN BORAX II AT 300 psig

	Result of Fourier analysis of the power	Value predicted by the theory of Appendix D
$\frac{\text{Fundamental's Amplitude}}{\text{Average Power}}$	.732	(normalized to .732)
$\frac{\text{2nd Harmonic's Amplitude}}{\text{Fundamental's Amplitude}}$	.407	.362
Phase between Fundamental and 2nd Harmonic	-105°	-99.5

III. TRANSFER FUNCTIONS

A. Theory

In the field of servomechanisms the theoretical and experimental analysis of a system in terms of its transfer function has proven to be valuable in understanding instabilities and designing away from them. As applied to a reactor, its transfer function is defined

$$G(\omega) = \frac{p/P^0}{k_{in}} \quad . \tag{3}$$

p/P^0 is a complex quantity containing the magnitude and phase of the oscillatory power amplitude ÷ average power caused by a driving oscillatory reactivity amplitude, k_{in}, with a frequency, $\omega/2\pi$. An equivalent, though more elegant and fundamental definition, is that $G(\omega)$ is the Fourier transform of the kernel, $B(\sigma)$, in the convolution,

$$p(t)/P^0 = \int_0^\infty B(\sigma)\, k_{in}(t-\sigma)\, d\sigma \quad . \tag{4}$$

From this it is also apparent that if k_{in} is a unit impulse or delta function, then the transfer function is the Fourier transform of the system's response, $B(t) = p(t)/P^0$.

Information about feedback processes affecting stability can be had by studying the deviation of $G(\omega)$ from its value at zero power, $G_0(\omega)$. If all feedback processes are lumped into $H(\omega)$, as in Fig. 10, one has from elementary feedback theory,[14]

$$G(\omega) = \frac{G_0(\omega)}{1 + G_0(\omega)\, H(\omega)} \quad . \tag{5}$$

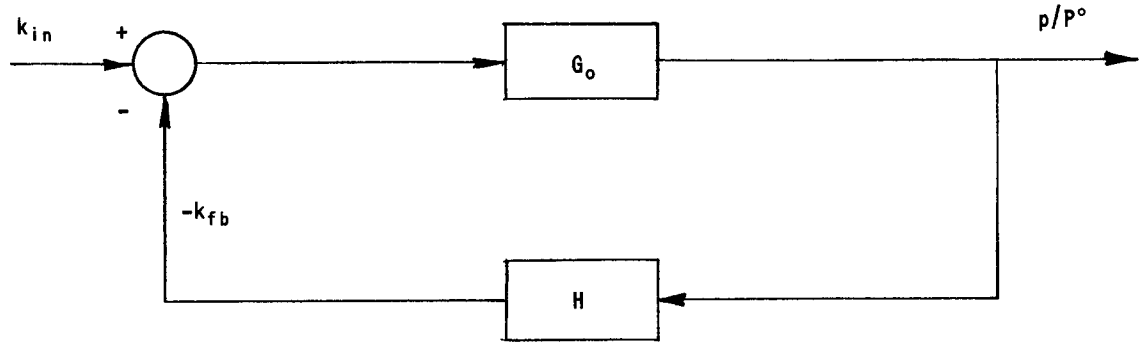

Fig. 10. Block Diagram of Reactor Feedback.

B. Control Rod Oscillator

The standard method of measuring the transfer function by sinusoidal oscillations of a control rod has been done on BORAX IV[9] and EBWR.[15] (Typical results are shown later in Fig. 20.) The height of the resonance found, as well as the resonant frequency increase with power is shown in Fig. 11.

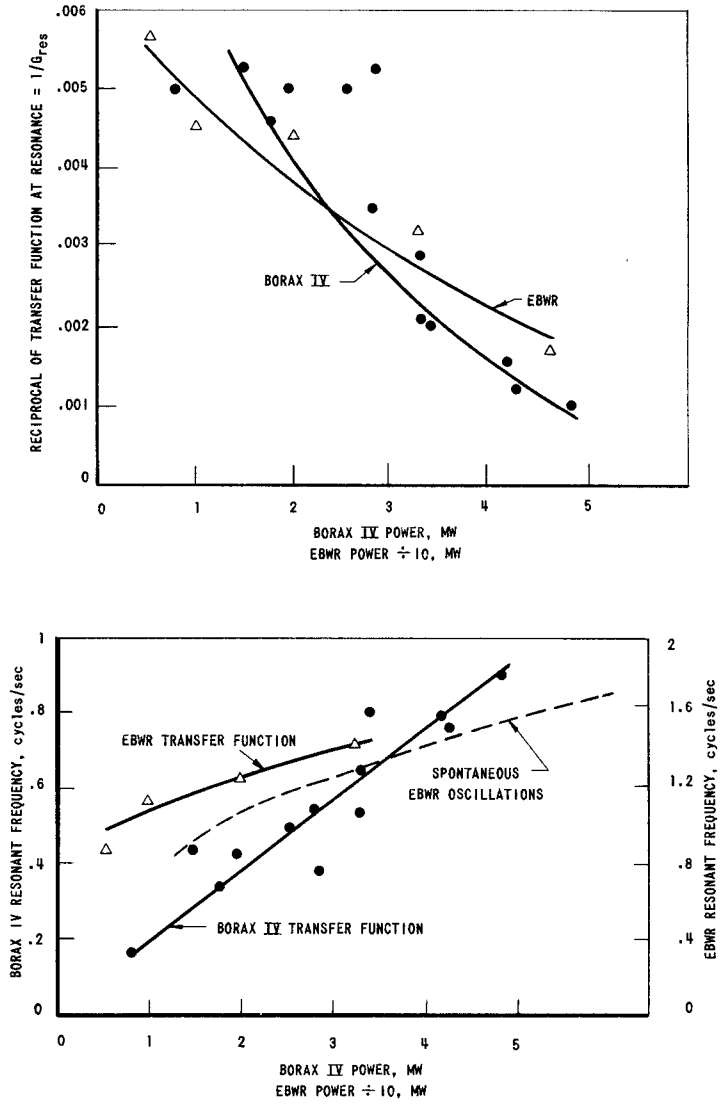

Fig. 11. Behavior of Maximum Resonant Value of the Transfer Function and its Resonant Frequency for BORAX IV at 0 psig and EBWR at 550 psig.

Using (5) it is possible to obtain H (ω) if G and G_0 are known. However unless the difference between G and G_0 is precisely known, large uncertainties in H can result. For the EBWR H was obtained with reasonable

precision,[16] but for BORAX IV only an approximate H could be found.[9] Because of the complex nature of the feedback process it is unlikely that this method can ever yield the precision required for a unique determination of the analytical form of H. However it can reasonably well evaluate constants in an assumed form of H. A more complete experimental understanding of the feedback process therefore requires transfer functions among all reactor variables in an extensively instrumented core.

In addition to providing information about feedback, it is hoped that transfer function measurements might offer a direct experimental tool in predicting unstable points from measurements at lower stable powers. Ideally this is accomplished by obtaining H (ω) from G (ω), and comparing with theories for H (ω). Depending on the accuracy of the theory, H (ω) can be extrapolated with more or less precision to values at higher powers, whence predictions of G (ω) are possible. Simpler, though less reliable, techniques are those of Figs. 11, 12, and 13. The latter two compare the resonant value of the transfer function with the oscillating fraction of the power of an undisturbed reactor having the same reactivity in steam voids at each point.

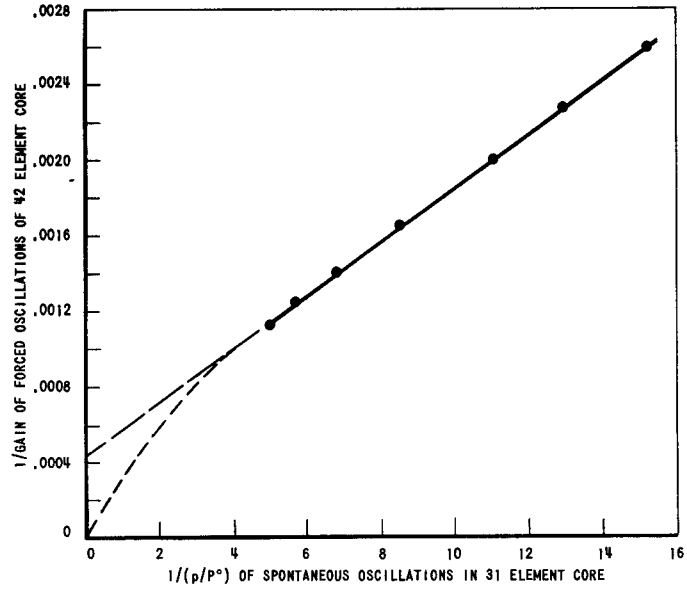

Fig. 12. Correlation of Spontaneous Oscillations with Transfer Function Measurements on BORAX IV at Atmospheric Pressure.

In ideal systems the transfer function is amplitude independent. However for reactors capable of self-sustained oscillations of finite amplitude, one expects the transfer function to be dependent upon the driving reactivity amplitude, at least in some region of operation.

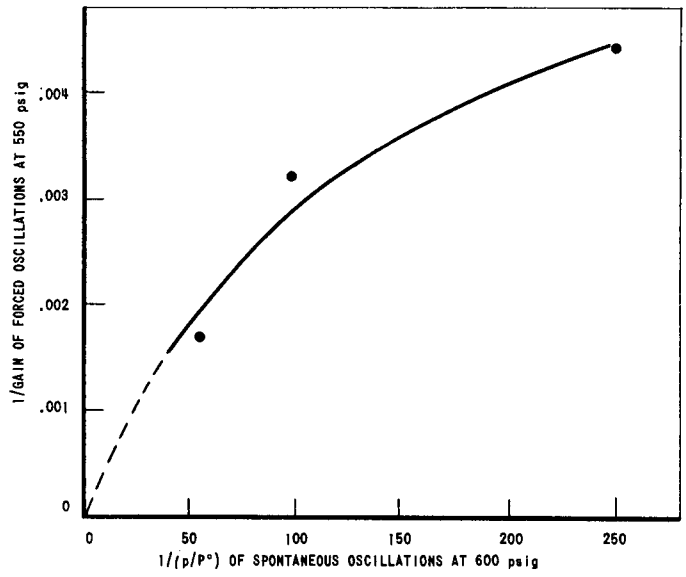

Fig. 13. Correlation of Spontaneous Oscillations with Transfer Function Measurements on EBWR.

C. Ringing

This type of test has been previously reported for reactors.[9] The name is derived from an analogy in acoustics, namely a damped sinusoidal response from a step input to a system, such as a loudspeaker. Bethe[17] has shown that the transfer function for a reactor disturbed by a reactivity step, k_0, at $t = 0$ is

$$G(\omega) = \frac{1}{P(0)k_0}\left\{P(\infty) - P(0) + i\omega\int_0^\infty [P(t) - P(\infty)]\, e^{-i\omega t}\, dt\right\} \qquad (6)$$

For sharp resonance with the maximum value of G at $\omega = \omega' >> \zeta\omega'$, this reduces to

$$G(\omega') \cong \frac{A}{2P(0)\zeta k_0} \qquad (7)$$

An approximate fit for $t > 0$,

$$P(t) \cong P(0) + A \sin(\omega t + \Phi)\, e^{-\zeta\omega' t} \qquad (8)$$

determine A and ζ.

Experiments of the type shown in Fig. 14 are analyzed by this simple procedure in Fig. 15. The discrepancy between ringing and rod oscillator measurements is in all probability due to experimental errors, although nonlinearities in the transfer function believed to occur at high resonant peaks make linear analysis increasingly erroneous.

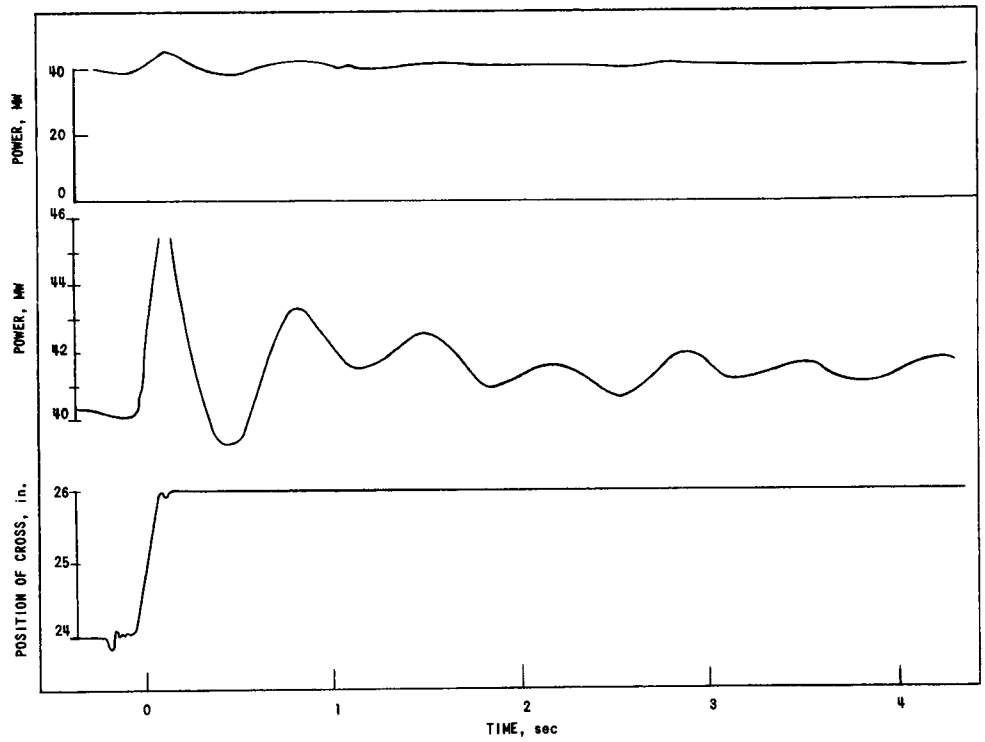

Fig. 14. Rapid Withdrawal of Two Inches of the Central Control Cross in EBWR at 40 MW and 600 psig.

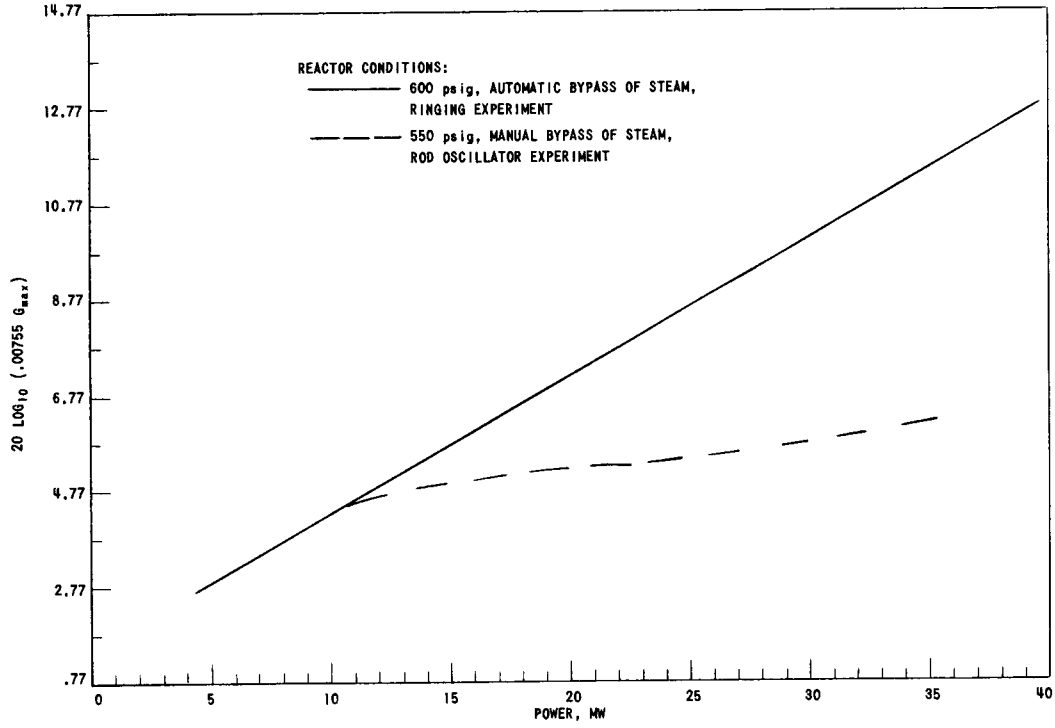

Fig. 15. The EBWR Transfer Function at the Resonant Frequency as Determined by Ringing and Rod Oscillation Experiments.

At the higher powers of Fig. 15 the reactor was in the small oscillatory condition. Even though a positive ζ is measured by ringing, the methods of Section II-A lead to ζ's which are sometimes instantaneously negative. Such behavior is not surprising in a nonlinear system under excitation by random noise.

D. Autocorrelation

It has been suggested[18] that information about a reactor's transfer function can be obtained by Wiener's theorem,

$$W(f) = \int_0^{\infty} \phi(\tau) \cos 2\pi f\tau \, d\tau \cong \int_0^{\tau_{max}} \phi(t) \cos 2\pi f\tau \, d\tau \qquad (9)$$

where $\phi(\tau)$ is the autocorrelation function of deviations of the reactor power from their mean value,

$$\phi(\tau) = \frac{\sum_{i=1}^{N} p(i\Delta t)\, p(i\Delta t + \tau)}{\sum_{i=1}^{N} p(i\Delta t)\, p(i\Delta t)} \,, \qquad (10)$$

$W(f)$ is the spectral density function, and $\sqrt{W(f)}$ is the Fourier amplitude of $p(t)$. The sampling interval, Δt, and the maximum lag, τ_{max}, determine the upper frequency limit and frequency resolution respectively.[19]

By definition of the transfer function,

$$\sqrt{W(f)} = |G(f)| \times \text{amplitude of frequency spectrum of the reactivity boiling noise at } f. \qquad (11)$$

Thus if the reactivity noise is relatively "white", (i.e. slowly varying with frequency), in the neighborhood of a resonance of G, the characteristics of this resonance can be obtained from $\sqrt{W}$. High "Q" resonances can be surveyed this way even if the reactivity noise source changes as much as 12 decibels per octave.

Figures 16 and 17 show results from analysis of power traces of BORAX IV and EBWR. When $\phi(\tau)$ can be approximated by a damped cosine function developing into random fluctuations, information about:

a) the resonance frequency, f', of the spectrum, W(f),
b) the resonant width, Δf, of W(f) at half maximum,

can be had directly from $\phi(\tau)$.

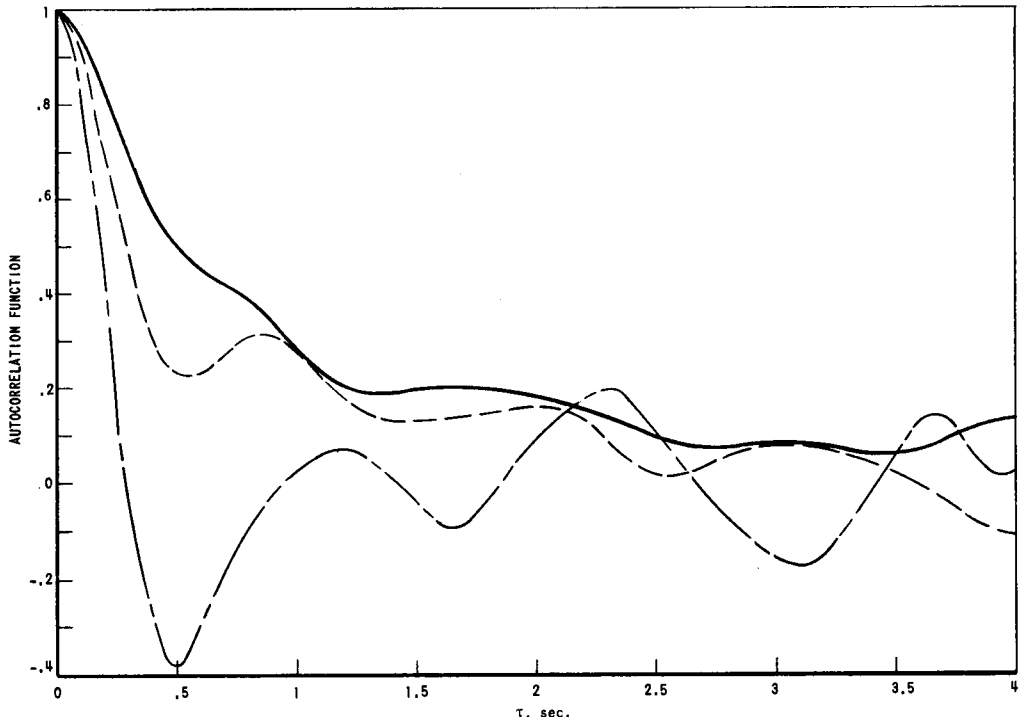

REACTOR	POWER, MW	PRESSURE, psig	τ_{max}, sec.	N	Δt, sec.
BORAX IV	4.18	0	5	200	.1
EBWR	20	550	10	1400	.05
EBWR	20	600	10	696	.1

Fig. 16. Autocorrelation Functions.

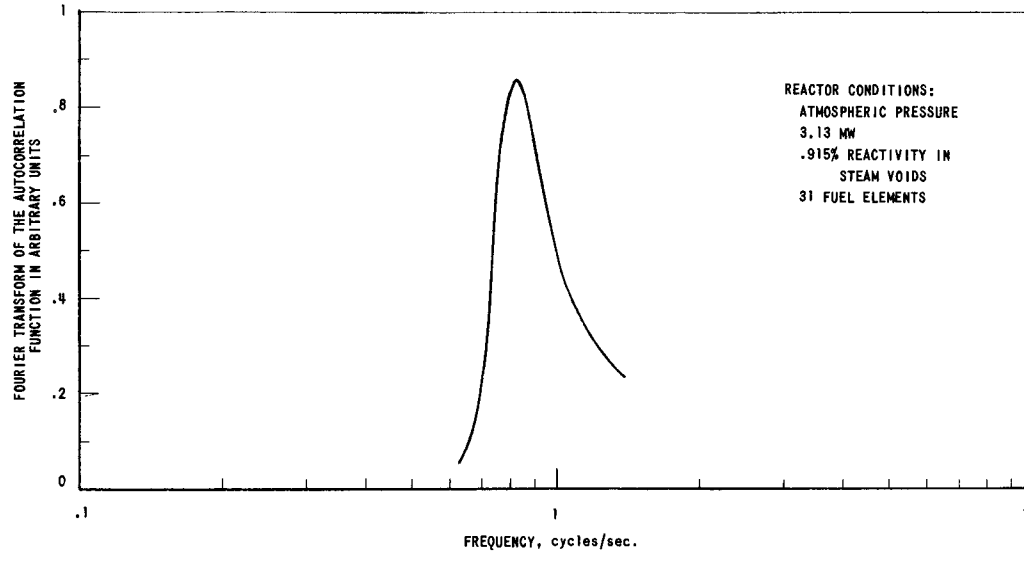

Fig. 17. Fourier Transform of $\phi(\tau)$ of Fig. 16.

$$\Delta f \equiv \frac{f'}{"Q"} = \frac{\omega'\zeta}{\pi} \quad , \tag{12}$$

where $\omega'\zeta$ is the damping constant of

$$\phi(\tau) \cong e^{-\omega'\zeta t} \cos \omega' t \quad . \tag{13}$$

The characteristics of the resonance of Fig. 17 are compared with transfer function measurements by the rod oscillator technique in Table VIII.

Table VIII

RESONANCE CHARACTERISTICS OF BORAX IV AND EBWR

	f' in cps	Δf in cps
BORAX IV		
From Fig. 17	.8	.32
From rod oscillator	.8	.44
EBWR		
From Fig. 16	1.2	(too broad to measure)
From rod oscillator	1.0	(too broad to measure)

Thus the autocorrelation method provides a method of obtaining information rather easily about the shape of a reactor's transfer function in the vicinity of a resonance.

IV. KINETICS THEORIES

A. Methods of Approach

The simplest procedure for interpretive analysis of experimental results presented here is completely empirical. Data can be correlated with little or no attempt at theorizing. Figures 12 and 13 are typical examples of this. Extrapolated predictions are possible by these methods, but are not accurate if extrapolations are large.

A somewhat more satisfactory analytical procedure is one using a phenomenological theory; i.e., one having equations describing the system using empirical constants which match the theory to the data. If the form of the equations is correct rather large extrapolated predictions are possible. Section IV-B uses this approach.

The ultimate, however, is a theory allowing a complete calculation of experimental results from basic considerations only. Sections IV-C and IV-D use this approach.

B. Phenomenological Feedback

The differential equations whose Laplace transform lead to the transfer function of Fig. 10 are:

$$\frac{p(t)}{P^0} = g_0 k(t) \tag{14}$$

$$k_{fb}(t) = -h \frac{p(t)}{P^0} \tag{15}$$

$$k(t) = k_{fb}(t) + k_{in}(t) \tag{16}$$

where g_0 and k are operators whose Laplace transforms are G(s) and H(s) respectively, and the former is related to $B_0(\sigma)$, the kernel of the linearized neutron kinetics equations:

$$g_0 k(t) = \int_0^\infty B_0(\sigma)\, k(t - \sigma)\, d\sigma \quad . \tag{17}$$

A fairly general discription for h is

$$h = \frac{\left[\prod_i \left(1 + T_{-i} \frac{d}{dt}\right)\right] \left[\sum_i \Lambda_i\, \delta(\tau_i, t)\right]}{\left[\prod_i \left(1 + T_i \frac{d}{dt}\right)\right] \left[\sum_i \Lambda_{-i} \delta(\tau_{-i}, t)\right]} \tag{18}$$

where the operator $\delta(\tau_i,t)$ is defined[20]

$$\delta(\tau_i,t)\, f(t) = f(t - \tau_i) \quad , \tag{19}$$

provided $f(t) = 0$ for $t < 0$.

Here Λ's are constants and the T's and τ's are time constants. Since

$$H(s) = \frac{\left[\prod_i \left(1 + T_{-i}s\right)\right]\left[\sum_i \Lambda_i \exp\left(-\tau_i s\right)\right]}{\left[\prod_i \left(1 + T_i s\right)\right]\left[\sum_i \Lambda_{-i} \exp\left(-\tau_{-i} s\right)\right]} \tag{20}$$

it is seen that Λ's are zero frequency feedback proportionality constants between p/P^0 and $-k_{fb}$. If the reactor transfer function is measured with sufficient precision, h or H can have all its parameters evaluated. For additional generality these parameters can even depend on p/P^0. The latter is necessary to explain self-sustained oscillations of finite amplitude.

The phenomenological approach has been found useful on the EBWR.[16] By assuming H to be of the form

$$H = \frac{\Lambda\left(1 + T_{-1}s\right)}{\prod_{i=1}^{4}\left(1 + T_i s\right)} \tag{21}$$

the 5 T's and Λ were determined as a function of power and pressure. Since Λ could be correlated with the slope of the power vs. reactivity in voids curve, and the T's are slowly varying with respect to power, it was possible to estimate H, (and therefore G) at 40 MW, using only data obtained at 20 MW or less.

C. Simplified Physical Model

In this section a model of boiling reactor dynamics will be assumed with the following characteristics:

a) deviations from equilibrium values of the reactor's variables are small, with linear differential equations being adequate. (This also implies $\delta(\tau,t)$ is approximated by a constant $\div\left(1 + T\,\frac{d}{dt}\right)$ in the frequency range of interest.)

b) effects stemming from pressure, water temperatures, coolant velocity, and steam velocity changes can be ignored. Feedback resulting from voids directly are therefore the only ones considered.

c) the nuclear importance of voids axially and radially, as well as the radial variation of other hydraulic and heat transfer quantities can be taken into account by the use of appropriate averages; i.e., power and flux distributions are taken to be flat both locally and over the entire reactor.

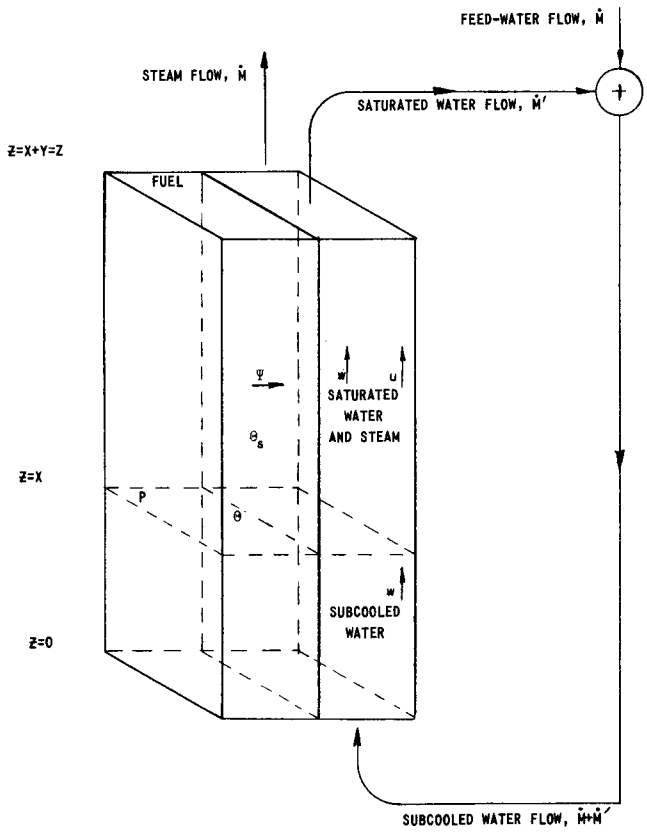

Fig. 18. Simplified Model Showing Basic Dynamic Processes

Figure 18 shows the basic processes therefore being assumed. The mass flow rates of steam, feedwater, and recirculatory water shown are respectively $\dot{M}$, $\dot{M}$, and $\dot{M}'$.

In the subcooled section the excess of $(P^0 + p)\Delta t/Z$, an energy impulse per unit height in the fuel, over $(\Psi^0 + \psi_w)\Delta t$, the heat transferred into the water per unit height, raises the temperature of the fuel and is therefore proportional to ψ_w, the deviation of the power transferred into the water per unit length, from its equilibrium value, $\Psi^0 = P^0/Z$.

$$\psi_w = \frac{1}{T_{1w}}\left(\frac{p\,\Delta t}{Z} - \psi_w\,\Delta t\right) \tag{22}$$

$$p = Z\left(1 + T_{1w}\frac{d}{dt}\right)\psi_w, \tag{23}$$

where the time constant, T_{1w}, lumps the effects of fuel, clad, and film. Similiarly in the boiling section,

$$p = Z\left(1 + T_{1b}\frac{d}{dt}\right)\psi_b \quad . \tag{24}$$

The Laplace transforms of (23) and (24) are

$$\frac{\psi_w(s)}{p(s)/P^0} = \frac{\Psi^0}{1 + T_{1w}s} \tag{25}$$

$$\frac{\psi_b(s)}{p(s)/P^0} = \frac{\Psi^0}{1 + T_{1b}s} \quad . \tag{26}$$

In a similar fashion the average fuel temperature rise, above saturation, $\Theta = \Theta^0 + \theta$, has four equations like (23) to (26):

$$p = \frac{P^0}{\Theta_w^0}\left(1 + T'_{1w}\frac{d}{dt}\right)\theta_w \tag{27}$$

$$p = \frac{P^0}{\Theta_b^0}\left(1 + T'_{1b}\frac{d}{dt}\right)\theta_b \tag{28}$$

$$\frac{\theta_w(s)}{p(s)/P^0} = \frac{\Theta_w^0}{1 + T'_{1w}s} \tag{29}$$

$$\frac{\theta_b(s)}{p(s)/P^0} = \frac{\Theta_b^0}{1 + T'_{1b}s} \tag{30}$$

The void volume per unit length, or steaming area, $A^0 + a$, in the water channel after an energy impulse per unit length, $(\Psi^0 + \psi_b)\Delta t$, deviates from its equilibrium value, A^0, because of a difference in the formation and exit rates per unit length.

$$\frac{\Psi^0}{\rho\ell} - \frac{\partial A^0}{\partial z}u = 0 \tag{31}$$

$$\frac{\psi_b}{\rho\ell} - \frac{\partial a}{\partial z}u = \frac{\partial a}{\partial t} \quad . \tag{32}$$

Here u, ρ, and ℓ are steam velocity, density, and latent heat of vaporization. If $z = X = X^0 + x$ is the instantaneous location of the boiling boundary, then the boundary condition becomes,

$$A^0(X^0 + x) + a(X^0 + x) = 0 \tag{33}$$

$$A^0(X^0) = 0 \tag{34}$$

$$\left(\frac{\partial A^0}{\partial z}\right)_{X^0} x + a(X^0) = 0 \quad . \tag{35}$$

Laplace transforming (33) and solving gives

$$a(s) = \frac{\psi_b(s)}{\rho\ell s}\left(1 - e^{-\frac{s(z-X^0)}{u}}\right) + a(X^0,s)e^{-\frac{s}{u}(z-X^0)}$$

$$= \frac{\psi_b(s)}{\rho\ell s}\left(1 - e^{-\frac{s(z-X^0)}{u}}\right) - \frac{\Psi^0 e^{-\frac{s}{u}(z - X^0)}}{\rho\ell u}x(s) \quad , \tag{36}$$

by virtue of (31) and (35). If the first and second terms of (36) are called $a_b(s)$ and $a_w(s)$ respectively, then

$$\frac{v_b(s)}{\psi_b(s)} = \int_{X_0}^{Z} \frac{a_b(s)}{\psi_b(s)}\,dz = \frac{Y^0}{\rho \ell s}\left\{1 - \frac{u}{sY^0}\left(1 - e^{-\frac{sY^0}{u}}\right)\right\}^{*} \quad . \tag{37}$$

To obtain the effect of boiling boundary shifts on voids by means of a_w it is necessary to solve the continuity equations in the subcooled region,

$$\Psi^0 - \dot{M}\frac{\partial C^0}{\partial z} = 0 \tag{38}$$

$$\psi_w - \dot{M}\frac{\partial c}{\partial z} = \frac{\dot{M}}{w}\frac{\partial c}{\partial t} \tag{39}$$

whose derivation is completey analogous to (31) and (32). Here $C^0 + c$ is the heat per unit mass of feedwater, whose velocity is w. The boundary conditions analogous to (34) and (35) are

$$c(0) = 0 \tag{40}$$

$$\left(\frac{\partial C^0}{\partial z}\right)_{X^0} x + c(X^0) = 0 \quad . \tag{41}$$

Laplace transforming (39) and solving using (40) gives

$$c(s) = \frac{w\psi_w(s)}{s\dot{M}}\left(1 - e^{-\frac{sz}{w}}\right) \quad , \tag{42}$$

From this, the Laplace transform of (38), and (41) one has

$$x(s) = -\frac{w\psi_w(s)}{s\Psi^0}\left(1 - e^{-\frac{sX^0}{w}}\right) \quad , \tag{43}$$

which after substitution into the second term of (36) gives

$$\frac{v_w(s)}{\psi_w(s)} = \int_{X^0}^{Z} \frac{a_w(s)}{\psi_w(s)}\,dz = \left[-\frac{\Psi^0}{\rho \ell s}\left(1 - e^{-\frac{sY^0}{u}}\right)\right]\left[-\frac{w}{s\Psi^0}\left(1 - e^{-\frac{sX^0}{w}}\right)\right] . \tag{44}$$

The required overall power to reactivity feedback transfer function is had by combining four feedbacks: $-(dk/d\theta_m)\,X^0/Z$ times (29) is the non-boiling zones fuel temperature effect; $-(dk/d\theta_m)\,Y^0/Z$ times (30) is the

*This result has also been obtained by T. Hamaguchi, Kyoto University, Japan (Private Communication).

boiling zone's fuel temperature effect; and -(dk/dv) times (44) X (25) and (37) X (26) are the void feedbacks from power generated in the non-boiling and boiling zones respectively.

$$H(s) = -\frac{dk}{d\theta_m}\left\{\frac{X^0}{Z}\frac{\Theta_w^0}{1+T'_{1w}s}+\frac{Y^0}{Z}\frac{\Theta_b^0}{1+T'_{1b}s}\right\}$$

$$-\frac{dk}{dv}\left\{\frac{w}{\rho\ell s^2}\left(1-e^{-\frac{sY^0}{u}}\right)\left(1-e^{-\frac{sX^0}{w}}\right)\frac{\Psi^0}{1+T_{1w}s}\right.$$

$$\left.+\frac{Y^0}{\rho\ell s}\left[1-\frac{u}{sY^0}\left(1-e^{-\frac{sY^0}{u}}\right)\right]\frac{\Psi^0}{1+T_{1b}s}\right\} \quad . \tag{45}$$

Here $dk/d\theta_m$ and dk/dv are overall average "metal" and void coefficients of reactivity respectively.

Figure 19 shows the block diagram of Fig. 10 with these explicit components of H. It is within the spirit of the approximations here to expand the exponentials and obtain

$$H(s) = -\frac{dk}{d\theta_m}\left\{\frac{Y^0}{Z}\frac{\Theta_b^0}{1+T'_{1b}s}+\frac{X^0}{Z}\frac{\Theta_w^0}{1+T'_{1w}s}\right\}$$

$$-\frac{dk}{dv}\frac{2T_{2b}}{\rho\ell}\left\{\frac{X^0\,\Psi^0}{(1+T_{2b}s)(1+T_{2w}s)(1+T_{1w}s)}\right.$$

$$\left.+\frac{\frac{1}{2}Y^0\,\Psi^0}{\left(1+\frac{2}{3}T_{2b}s\right)\left(1+T_{1b}s\right)}\right\} \quad , \tag{46}$$

where $T_{2b} = Y^0/2u$ and $T_{1w} = X^0/2w$ are average transit times of steam and subcooled water. The system of linear differential equations which also has (46) as their transform consists of (23), (24), (27), (28) and the following:

$$\frac{Y^0 T_{2b}}{\rho\ell}\psi_b = \left(1+\frac{2}{3}T_{2b}\frac{d}{dt}\right)v_b \tag{47}$$

$$-\frac{X^0\psi_w}{\Psi^0} = \left(1+T_{2w}\frac{d}{dt}\right)x \tag{48}$$

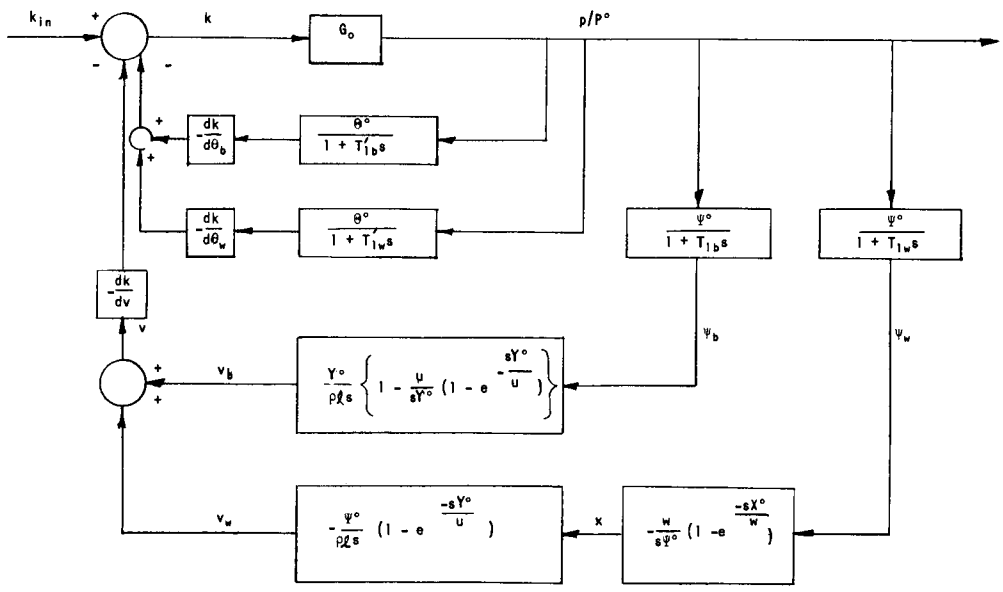

Fig. 19. Mathematical Model of the Reactor Transfer Function

$$-\frac{2T_{2b}\Psi^0}{\rho\ell}\,x = \left(1 + T_{2b}\frac{d}{dt}\right)v_w \tag{49}$$

$$k_{fb} = \frac{dk}{d\theta_m}\left(\frac{Y^0}{Z}\theta_b + \frac{X^0}{Z}\theta_w\right) + \frac{dk}{dv}(v_b + v_w) \quad . \tag{50}$$

In this simplified form the physical interpretations of the processes (47), (48), and (49) are analogous to those of (25), and (26): the excess of the production rate of a variable over the variable divided by a time constant is equal to the time rate of change of the variable.

A reasonable approach to Section IV-B's phenomenological interpretation of boiling reactor dynamic behavior over a limited frequency region would be to consider equations (25), through (28) and (47) through (50) as representative of the important processes, but with adjustable parameters, since the approximations and assumptions made above lead to admittedly uncertain values for the parameters. This suggests a 6 parameter formulation of H, (when metal temperature feedbacks can be ignored):

$$H(s) = \frac{\Lambda_w}{(1 + T_{2b}s)(1 + T_{2w}s)(1 + T_{1w}s)} + \frac{\Lambda_b}{\left(1 + \frac{2}{3}T_{2b}s\right)\left(1 + T_{1b}s\right)} \tag{51}$$

where T_{2b} and T_{2w} are arbitrary and not necessarily $Y^0/2u$ and $X^0/2w$ respectively. Both EBWR and BORAX IV transfer function data readily admit such interpretation, however, neither are sufficiently precise to demonstrate the uniqueness of any interpretation.

D. Calculated Transfer Functions

An Argonne program, (BUM), made possible IBM 650 or 704 computation of reactor transfer functions using (46) from feedback time constants. The latter, given in Table IX, were determined from the data of Appendixes B and C. It should be stressed that, except for dk/dv, all constants used were obtained entirely from basic calculations and out-of-pile measurements. The void coefficient, dk/dv, was obtained from the reactor's measured steady state reactivity in voids and its void volume fraction computed from theory. (Appendix B indicates that dk/dv calculated by reactor statics is generally in fair agreement with experiments anyway.) $dk/d\,\theta_m$ effects were neglected in the numerical calculations. Since feedbacks stemming from pressure changes[21] are omitted for simplicity in the above theory, the validity of the results is restricted to the higher frequencies shown in Figs. 20 and 21.

Table IX

CONSTANTS IN (51) USED IN COMPUTING REACTOR TRANSFER FUNCTIONS

Reactor	Pressure in psig	Power in MW	Λ_b	Λ_w	T_{1b} in sec	T_{2b} in sec	T_{2w} in sec	T_{1w} in sec
EBWR	600	20	.00960	.01228	.351	.183	.1757	.445
EBWR	300	20	.01205	.01343	.354	.1322	.1475	.485
EBWR	600	5.4	.00282	.003604	.429	.2134	.2049	.631
EBWR	600	50	.02588	.03307	.328	.1775	.1711	.389
BORAX II*	77	3.85	.0693	.0616	.0522	.1467	.1272	.180
BORAX II*	150	3.85	.0574	.0583	.0479	.1526	.1428	.164
BORAX II*	300	4.985	.0635	.0754	.0250	.1637	.1695	.072
BORAX III	300	7.13	.01035	.01231	.0564	.1359	.127	.149
BORAX III	300	14.24	.03238	.03858	.0249	.1128	.1102	.072
BORAX IV**	300	6.31	.02538	.02835	.491	.1081	.0988	.582
BORAX IV**	300	12.26	.03940	.04395	.376	.0932	.0904	.422

*55 element loading **59 element loading

For EBWR, where direct comparison with experiment is possible, the results are very encouraging to the theory presented here. Also shown are the results of an older theory[22] having only two feedback time constants. For the BORAX reactors, no transfer function measurements were made at the higher pressures. Nevertheless, the height of the transfer function's resonance displays the same trends observed by oscillating threshold measurements in Table VI. It is theorized that in the presence of random excitation by "boiling noise," a sharply resonant transfer function (rather than one of infinite value) is a sufficient condition to allow small oscillatory behavior.

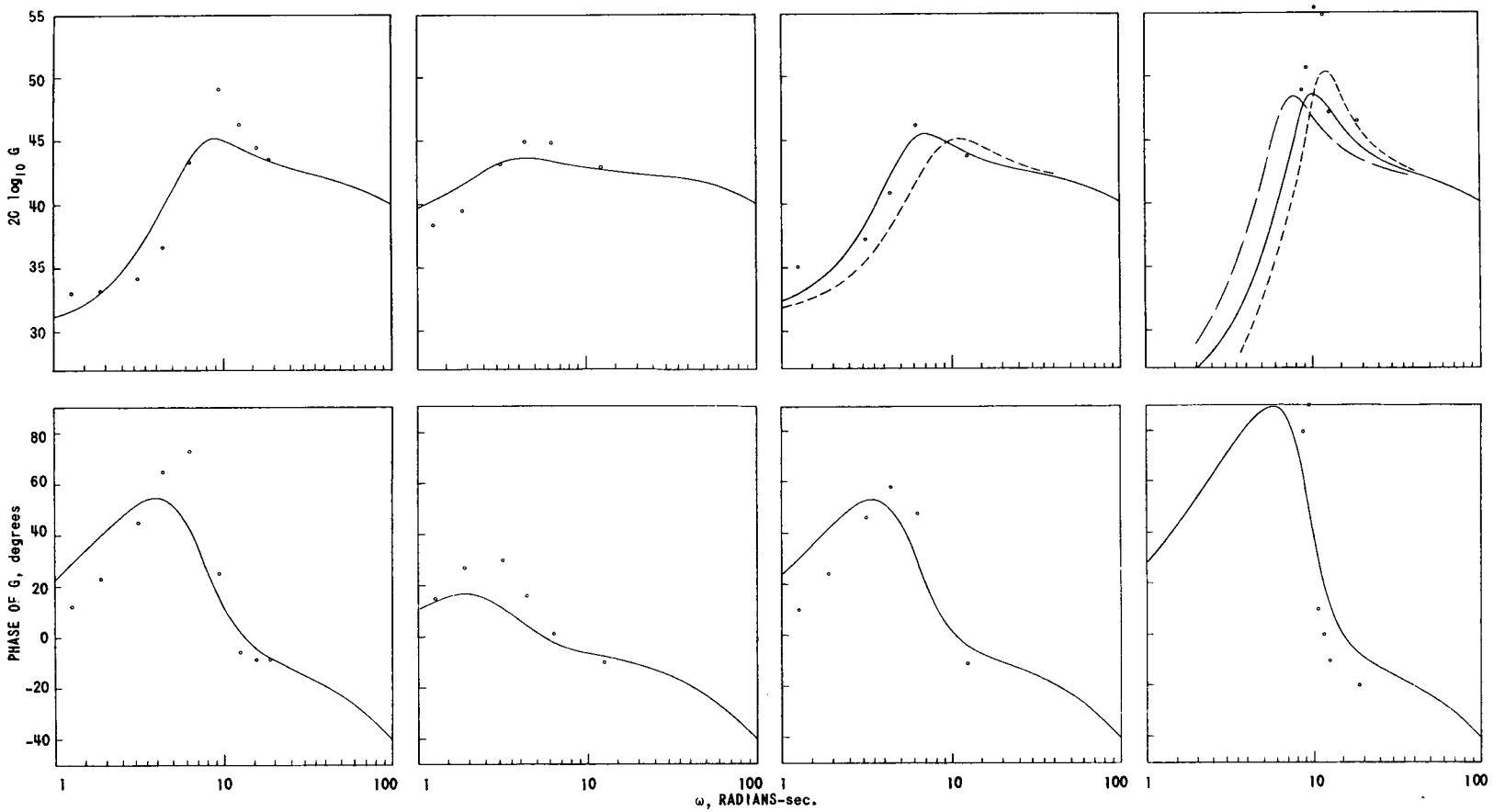

	—— °	—— °	—— ---(1) °	—— ——(2) - - - -(3) °
PRESSURE, psig	300 305	600 550	600 600 550	600 600 600 600
POWER, MW	20 19.9	5.4 5.4	20 20 19.9	50 50 50 50

(1) USES ORIGINAL TWO-TIME-CONSTANT THEORY (ANL-5601)
(2) ALL TIME CONSTANTS ARBITRARILY INCREASED BY A FACTOR OF 1.8 BEFORE USE
(3) dk/dv ARBITRARILY MULTIPLIED BY 1.5 BEFORE USE

Fig. 20. Comparison of Calculated Transfer Functions with Experimental Points for the EBWR

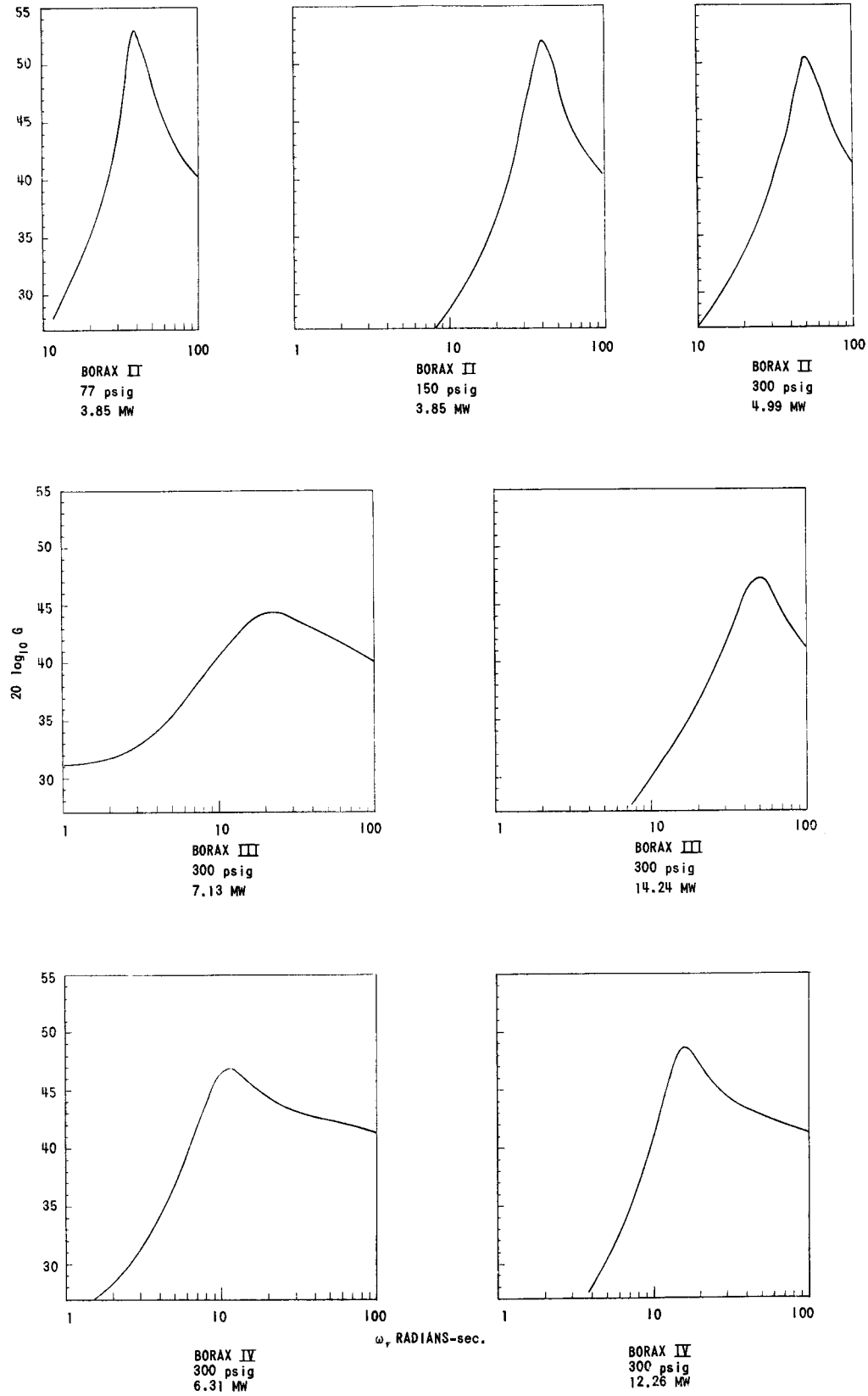

Fig. 21. Transfer Functions Calculations for the Borax Reactors

The theoretical results of Figs. 20 and 21 also show the dependence of resonant frequency on power found experimentally in Section II-C. Apparently, the basic constants in the theory are not as well known for the BORAX-II and III reactors. These have resonant frequencies somewhat higher than observed.

E. Hydraulic Instability

It has been demonstrated experimentally[23,24] that electrically heated natural circulation boiling loops are capable of self-induced oscillations in spite of the apparent lack of any feedback to the loop's steady electrical power. Furthermore, these oscillations have frequencies in the .5 to 1.5 cps range and occur at power densities comparable to those encountered in reactors which are oscillatory.

These data suggest that H(s) of Fig. 10 can be a resonant function under certain conditions. For positive real time constants, (46) has no such behavior. However, the more general formula, (20), can readily accommodate this, for example, by a pair of complex conjugate T_i's:

$$H = \frac{1}{\left[1 + \frac{1}{\omega_0}\left(\zeta - j\sqrt{1-\zeta^2}\right)s\right]\left[1 + \frac{1}{\omega_0}\left(\zeta + j\sqrt{1-\zeta^2}\right)s\right]} \quad , \qquad (52)$$

where ω_0 and 2ζ are the resonant angular frequency and reciprocal "Q" respectively.[25]

It is quite possible that these hydraulic oscillations, rather than being capable of description by linear theory, actually depend on nonlinearities for their existence even at small amplitudes. In this case to retain (52), probably requires strongly amplitude dependent time constants. (Transfer functions measurements on electrically heated loops are underway at Argonne and Ramo-Wooldridge. These should shed light on this point.)

If hydraulic instabilities of this type occur in reactors, the reactor could act merely as a water density meter, i.e., no feedback through reactor power is required to sustain hydraulic oscillations. So far there is no conclusive proof that hydraulic instabilities have occurred in EBWR or BORAX, (although the type B oscillation of Section II - G is speculatively considered to be hydraulic). On the other hand the model of Section IV - C seems to be supported by much EBWR and BORAX data.

F. Flux Tilt Instability

In addition to the types of instabilities already observed:

Type A of Section II-G
Type B of Section II-G
Hydraulic instability of Section IV-E

another is speculatively proposed in this section. It is conceivable that in large, low-leakage reactors with large reactivities in voids, an oscillating flux shape at constant power (analogous to xenon instability) might develop. The cycle would be the following: A power surge in half, A, of the reactor increases the voids there; the subsequent lowering of material buckling in that region terminates the surge and lowers the flux and power to a sub-normal value. To remain at constant total power, the power in the other half, B, of the reactor rises. The initial condition of the cycle is again had when the voids have escaped from A, and increased in B, to induce the flux and power distribution initially had.

To date boiling reactors have been small and have not been internally monitored for flux tilting. Therefore no evidence exists of this instability. Theoretical work, however, is in progress.(26)

V. CONCLUSIONS

The most commonly observed type of boiling water reactor oscillations has had extensive experimental investigation. From detailed analyses of power, pressure, and temperature measurements, the properties of these oscillations have been determined in great detail. Transfer function measurements have succeeded in obtaining an even better quantitative description of the reactor's dynamic behavior. Auto-correlation techniques have been found to give, at least approximately, information similar to that obtained by the laborious transfer function measurements.

A theory which satisfactorily describes quantitatively this type of oscillation has been developed. The two chief feedbacks which cause the reactor's resonant behavior are: steam void fluctuations due to power generated in the boiling zone, and boiling boundary fluctuations due to power generated in the non-boiling zone.

Other types of instability were discussed, but currently lack any quantitative theoretical understanding. Since their occurrence seems to be rare, it is probably sufficient to incorporate only considerations of the better understood type of instability into boiling reactor designs. Having available now a method of calculating a reactor's resonant characteristics, it can be used to optimize design by influencing the choice of time constants and void coefficients. Thus it should be possible for boiling reactors to exceed current performance, which is about 50 kilowatts per litre of core.

VI. ACKNOWLEDGEMENTS

BORAX data discussed have been obtained under the direction of H. V. Lichtenberger, M. Novick, and R. Wallin, and EBWR data by J. M. Harrer and J. A. deShong. Numerical calculations associated with analysis of experiments and evaluation of theories were made with the assistance of E. Fabricius and S. Jacobs. The use of the IBM - 650 and 704 was possible with the cooperation of C. Cohn and computing group under M. Butler. A greater insight into the feedback mechanisms was had from the efforts of Z. Akcasu.

REFERENCES

1. W. M. Breazeale, T. E. Cole and J. A. Cox, "Preliminary Boiling Experiments in the LITR," Reactor Sci. Tech. 2 (2) 173 (Aug. 1952).

2. W. M. Breazeale, T. E. Cole and J. A. Cox, "Further Boiling Experiments in the LITR," Reactor Sci. Tech, 2 (4) 186 (Dec. 1952).

3. S. G. Forbes, F. Schroeder and W. E. Nyer, "First Reports on Instability in SPERT I," Nucleonics 15, No. 1, 41 (1957).

4. J. A. Thie, "Boiling Water Reactor Instability," Nucleonics 16 - 3, 102 (1958).

5. J. R. Dietrich, D. C. Layman and O. A. Schulze, "The Proposed Boiling Reactor Experiment," ANL-4921, Nov. 12, 1952.

6. J. R. Dietrich and D. C. Layman, "Transient and Steady State Characteristics of a Boiling Reactor," ANL-5211, February, 1954.

7. J. R. Dietrich, H. V. Lichtenberger and W. H. Zinn, "Design and Operating Experience of a Prototype Boiling Water Power Reactor" 1955 Geneva Conference, 8/P/851.

8. W. H. Zinn, et al., "Operational Experience with the BORAX Power Plant," Nuc. Sci. and Eng. 1, 420 (1956).

9. B. Maxon, O. A. Schulze, and J. A. Thie, "An Experimental Investigation of Reactivity Transients and Steady State Operation of the BORAX IV Boiling Reactor," ANL-5733.

10. O. A. Schulze, "BORAX IV Operation - Atmospheric Pressure," ANS Pittsburgh Meeting, June 1957.

11. "The EBWR, Experimental Boiling Water Reactor," ANL-5607 (1957).

12. J. A. Thie, "EBWR Physics Experiments," ANL-5711 (1957).

13. "VBWR on the Line," Nucleonics 16-2, 76 (1958).

14. W. Chestnut & R. Mayer, "Servomechanisms and Regulating System Design," Wiley, N. Y., 1951, pg 139.

15. J. A. deShong, "Power Transfer Functions of the EBWR Obtained Using a Sinusoidal Reactivity Driving Function," ANL-5798 (1957).

16. J. A. deShong, Jr., "Upping EBWR's Power," Nucleonics 16 - 6, 68 (1958).

17. H. A. Bethe, APDA-117

18. M. N. Moore, "The Determination of Reactor Transfer Functions from Measurements at Steady Operation," Nuc. Sci. Eng: 3, 387 (1958).

19. R. B. Blackman & J. W. Tukey, "The Measurement of Power Spectra," Bell Syst. Tech. Jonl, 37, No. 2, 485 (1958).

20. H. Margenau & G. Murphy, "The Mathematics of Physics and Chemistry," Van Nostrand (1956).

21. E. Beckjord, "Dynamic Analysis of Natural Circulation Boiling Water Power Reactors," ANL-5799 (1958).

22. J. A. Thie, ANL-5601, (1956) pg 31.

23. A. S. Jameson & P. A. Lottes, "Natural Circulation Boiling of Water Flowing Upward Through an Annulus," ANL-5208, p.150 (1953).

24. W. H. Cook and J. F. Marchaterre, "Single & Multi-Channel Natural Circulation Boiling at 600 psig," ANL-5561 p.60 (1955).

25. H. Chestnut and R. Mayer, "Servomechanisms and Regulating System Design," Wiley, N. Y., 1951, pg 310.

26. T. Snyder, (Private Communication), G. E. Vallecitos.

APPENDIX A

Reactor Mechanical Data

by J. A. Thie

BORAX I (see reference 6)

BORAX II

Core Size (Rectangular Parallelopiped)

Number of fuel elements	$4N_{\parallel} \times N_{\perp}$
Length parallel to fuel plates	$.75 + 6.118\ N_{\parallel}$ inches
Length perpendicular to fuel plates	$.75 + 6.586\ N_{\perp}$ inches
Height of fuel	23.625 inches
Riser height above fuel	2 inches
Non-fueled height below fuel	7 inches

Fuel Element

Thickness of water channel	.264 inches
Width of water channel (before curving)	2.845 inches
Thickness	
U^{235}~Al center	.020 inches
Clad on each side	.020 inches
Total	.060 inches
No. of plates per fuel element	10
Amount of fully enriched U^{235} per fuel element	
"Heavies"	157.3 gms
"Lights"	93.4 gms
Heat transfer area per fuel element	8.3 ft^2
Coolant volume (exclusive of control channels) per fuel element	2.80 litres

Reactor Vessel

Inside diameter	52.5 inches
Height	16 ft
Thickness	3/4 inches

BORAX III (see reference 7)

Core Size

Number of fuel elements	87
Radius of equivalent cylinder	54.04 cm
Fuel height	65.53 cm
Riser height above fuel	23 inches
Non-fueled height below fuel	7 inches

Fuel Element

Thickness of water channel	.264 inches
Width of water channel	1.72 inches
Thickness	
U^{235}~ Al center	.020 inches
Clad on each side	.020 inches
Total	.060 inches
No. of plates per fuel element	24
Amount of fully enriched U^{235} per fuel element	
"Heavies"	225 gms
"Lights"	133 gms
Heat transfer area per fuel element	15.04 ft^2
Coolant volume (exclusive of control channels) per fuel element	4.852 litres

Reactor Vessel (same as BORAX II)

BORAX IV (see reference 9)

Core Size (Rectangular Parallelopiped)

Number of fuel elements	4 $N_{\parallel}$ x $N_{\perp}$
Length parallel to fuel plates	.875 + 8 $N_{\parallel}$ inches
Length perpendicular to fuel plates	.875 + 7.776 $N_{\perp}$ inches
Height of fuel	24-3/8 inches
Riser height above fuel	23 inches
Non-fueled height below fuel	7 inches

Fuel Element

Equivalent thickness of water channel	.472 inches
Width of water channel	3.684 inches

Fuel Element (continued)

Outside diameters	
Oxide fuel rods	.23 inches
Lead bond	.266 inches
Cladding	.298 inches
No. of fuel rods per fuel element	47
Amount of fully enriched U^{235} per fuel element	283 grams
Amount of $ThO_2 + UO_2$ per fuel element	5524 grams
Heat transfer area per fuel element	7.566 ft^2
Coolant volume (exclusive of control channels) per fuel element	4.33 litres

Reactor Vessel (same as BORAX II)

EBWR (see reference 11)

APPENDIX B

Reactor Physics

by J. A. Thie

BORAX I (see reference 6)

BORAX II

	48 Light Elements	59 Light Elements		67 Light Elements
	63°F.	63°F.	421°F.	421°F.
L^2 in cm^2	4.68	4.68	10.00	10.00
$\overline{\Sigma}_a = Ds/L^2$ in cm^{-1}	.04695	.04695	.03369	.03369
τ in cm^2	46.34	46.34	62.20	62.20
Reflector Savings in cm	7.00	7.00	8.84	8.84
B^2 in cm^{-2}	.005639	.005019	.004573	.004299
$k_\infty = \eta^{25} f = 2.094 f$	1.3603*	1.3603*	1.4064*	1.4064*
$1 - (1 + L^2B^2) \exp(\tau B^2)/k_\infty$	.0200	.0506	.0118	.0313
Experimental Reactivity	.00285	-	.00855	.0329
Neutron lifetime in sec.	7.5×10^{-5}	7.5×10^{-5}	-	-
kg of U^{235}	4.48	5.51	5.51	6.26
Void coefficient	-	-	-	-.19

*no xenon or samarium

BORAX III

Temperature in °F.	62.5	421	421
Percentage Steam Voids	0	0	20
L^2 in cm^2	4.27	9.11	13.03
$\overline{\Sigma}_a = Ds/L^2$ in cm^{-1}	.0507	.0365	.0347
τ in cm^2	45.04	60.55	89.00
Radial reflector savings in cm	6.9	8.73	10.60

BORAX III (continued)

	48 Light Elements	59 Light Elements		67 Light Elements
	63° F.	63° F.	421° F.	421° F.
B^2 in cm^{-2}		.003311	.003112	.002921
$k_\infty = \eta^{25} f = 2.094\ f$		1.3006*	1.3388*	1.4076*
$\rho = 1 - (1 + L^2B^2)\ \exp(\tau B^2)/k_\infty$		.0948	.0728	.0436
Experimental ρ		-	.0671	-
neutron lifetime in sec.		6.7×10^{-5}	-	-

*virgin reactor; no xenon nor samarium

BORAX IV (see reference 9)

EBWR (see reference 12)

Reactivities in steam voids:

Reactor	No. of Elements	Pressure in psig	Power in MW	Average void coefficient from reactor physics	Average Percentage voids in coolant from reactor hydraulics	Percent Reactivity in voids	
						Calculated	Measured
BORAX II	67	300	5.78	-.19	13.4	2.6	2.67
BORAX III	87	300	12.5	-.10	9.65	1.0	1.67
BORAX IV	59	300	6.3	-.28	9.95	2.8	3.00
BORAX IV	59	300	12.26	-.28	14.5	4.1	5.05
EBWR	114	600	19.62	-.10	7.7*	.8	.72

*From reference 12

APPENDIX C

Reactor Hydraulics

by J. Marchaterre

The reactor hydraulics parameters believed to have an influence on boiling reactor stability are: average coolant void fraction, $\bar{\alpha}$; exit coolant void fraction, α_{ex}; the ratio of boiling length to total heated length, L_B/L_T; coolant velocity at the inlet, v_i; and the slip ratio, R = steam velocity ÷ coolant velocity. These quantities can be had by well established techniques* of natural circulation boiling analysis if the geometry, feedwater temperature, pressure, and power conditions are specified. The table below gives the results of such calculations for fuel elements of various reactors under various conditions.

Reactor	Pressure psig	Power in one fuel element	Feedwater temp	$\frac{L_B}{L_T}$	Inlet velocity fps	Average void in coolant channel	α_{ex} (avg)	Velocity ratio R
BORAX I	0	15	203	1	0.96	0.55	0.77	1.95
BORAX I	0	30	203	1	1.60	0.73	0.89	3.0
EBWR	600	44.65	130	0.61	2.60	0.036	0.105	1.50
EBWR	600	89.3	130	0.61	3.15	0.058	0.160	1.50
EBWR	600	178.5	130	0.61	3.90	0.092	0.260	1.50
EBWR	600	268	130	0.61	4.25	0.125	0.330	1.50
EBWR	600	3.57	130	0.61	4.50	0.145	0.380	1.51
EBWR	600	446.5	130	0.61	4.55	0.165	0.420	1.51
EBWR	600	536	130	0.61	4.62	0.185	0.460	1.51
BORAX II	77	35	75	.692	2.36	.166	.41	1.75
BORAX II	77	70	75	.692	2.42	.242	.55	1.95
BORAX II	150	11.67	75	.663	1.68	.063	.17	1.57
BORAX II	150	35	75	.663	2.16	.126	.31	1.68
BORAX II	150	70	75	.663	2.36	.172	.44	1.84
BORAX II	300	90.7	75	.627	2.20	.138	.38	(1.74)
BORAX III	300	81.9	75	.627	3.16	.069	.20	1.57
BORAX III	300	163.7	75	.627	3.64	.1035	.29	1.64
BORAX III	300	163.7	116	.645	3.64	.105	.295	1.64
BORAX IV	0	124	75	.778	1.82	.623	.91	2.76
BORAX IV	0	132.1	109	.811	1.81	.645	.92	2.78
BORAX IV	250	10.54	109	.652	2.04	.0228	.07	1.5
BORAX IV	250	30.48	109	.652	2.88	.0522	.145	1.54
BORAX IV	250	57.4	109	.652	3.32	.075	.21	1.58
BORAX IV	250	90.7	109	.652	3.68	.099	.27	1.62
BORAX IV	250	176	109	.652	4.08	.147	.385	1.74
BORAX IV	250	291.6	109	.652	4.16	.192	.48	1.92
BORAX IV	300	12.59	109	.642	1.95	.0225	.07	1.54
BORAX IV	300	39.04	109	.642	2.82	.0514	.145	1.58
BORAX IV	300	67.7	109	.642	3.32	.077	.215	1.60
BORAX IV	300	106.9	109	.642	3.68	.0995	.280	1.64
BORAX IV	300	207.8	109	.642	4.02	.145	.385	1.74
BORAX IV	300	342.8	109	.642	4.12	.194	.49	1.90
BORAX IV	300	124	75	.627	3.78	.107	.30	1.66

*P. A. Lottes & W. S. Flinn, Nuc. Sci. & Eng. 1, 461 (1956)

APPENDIX D

Derivation of Harmonic Content in the Power Due to a Sinusoidal Reactivity Variation

by J. A. Thie

An exact solution of the reactor kinetics equations having a sinusoidal power fluctuation,

$$N(t) = \frac{N_0}{2} + N_1 \sin \omega t \tag{1}$$

has been shown by Greenspan* to be

$$k_{ex}\left(\frac{N_0}{2} + N_1 \sin \omega t\right) = \frac{N_1}{|G_1|} \sin (\omega t - \psi_1) \tag{2}$$

where

$$|G_1|\ e^{j\psi_1} = \frac{1 - j\omega \sum_i \frac{\beta_i}{\lambda_i + j\omega}}{j\omega \left(\ell + \sum_i \frac{\beta_i}{\lambda_i + j\omega}\right)} \tag{3}$$

Also, if

$$N(t) = \frac{N_0}{2} + N_2 \sin (2\omega t + \phi) \tag{4}$$

then

$$k_{ex}\left[\frac{N_0}{2} + N_2 \sin (2\omega t + \phi)\right] = \frac{N_2}{|G_2|} \sin (2\omega t + \phi - \psi_2) \tag{5}$$

Since the kinetics equations are linear in the functions N and k_{ex} N, these solutions can be added.

$$N(t) = N_0 + N_1 \sin \omega t + N_2 \sin (2\omega t + \phi) \tag{6}$$

corresponds to, from (2) and (5),

$$k_{ex} = \frac{\frac{N_1}{|G_1| N_0} \sin (\omega t - \psi_1) + \frac{N_2}{|G_1| N_0} \sin (2\omega t + \phi - \psi_2)}{1 + \frac{N_1}{N_0} \sin \omega t + \frac{N_2}{N_0} \sin (2\omega t + \phi)} \tag{7}$$

---

*ANL - 5577 pg 26

If $N_2 << N_1 << N_0$, then the conditions for k_{ex} to consist only of one frequency,

$$k_{ex} \cong \frac{N_1}{|G_1| N_0} \sin(\omega t - \psi_1) - \frac{N_1^2}{2|G_1| N_0^2} \cos \psi_1 \tag{8}$$

are

$$\frac{N_2}{N_1} = \frac{1}{2} \left(\frac{N_1}{N_0}\right) \frac{|G_2|}{|G_1|} \tag{9}$$

and

$$\phi = \psi_2 - \psi_1 - \pi/2 \tag{10}$$

APPENDIX E

Generalized Theory of Feedback

by

Z. Akcasu and J. A. Thie

In section IV - C it was assumed that appropriate reactor averages could be used for many quantities and that single time constants can be used to approximate complicated functions over a limited range. Here not only will these approximations be eliminated but additional effects stemming from pressure and feedwater variations will be taken into account.

The Laplace transform solution to the heat transport equations in two regions, (fuel and clad), one of which has uniform heat generation, is quite straightforward in both one-dimensional slab and cylindrical geometry. Only the results are presented, and they are for the following boundary conditions:

1. Symmetry about the fuel's center.
2. Continuity of temperature and heat flow at the fuel-clad interface.
3. The power transferred into the water per unit area of surface is a [excess of surface temperature over water temperature]$^{\eta}$, where a and η are empirical constants.

For slabs,

$$\frac{\psi(s)/\Psi^0}{p(s)/P^0} = \frac{\sinh \sqrt{\tau_1 s}}{\sqrt{\tau_1 s}} \left[\frac{\sqrt{\tau_1 s}}{R_1} (\sinh \sqrt{\tau_1 s}) \cdot \left(R_2 \frac{\sinh \sqrt{\tau_2 s}}{\tau_2 s} + R_3 \cosh \sqrt{\tau_2 s} \right) + (\cosh \sqrt{\tau_1 s}) \cdot \left(\cosh \sqrt{\tau_2 s} + \frac{R_3}{R_2} \sqrt{\tau_2 s} \sinh \sqrt{\tau_2 s} \right) \right]^{-1} .$$

The time constants of the fuel and clad are respectively,

$$\tau_1 = c_1 \delta_1^2 / k_1$$

$$\tau_2 = c_2 \delta_2^2 / k_2$$

where c, k and δ are specific heat, conductivity, and thickness traversed by the heat, (i.e., fuel half-thickness, and clad thickness). The thermal resistances of fuel, clad, and film are respectively,

$$R_1 = \delta_1/k_1$$

$$R_2 = \delta_2/k_2$$

R_3 = Excess of surface temperature over water temperature ÷ (η x power per unit area of surface).

Also the transfer function for the average slab fuel temperature is

$$\frac{\theta(s)/\Theta^0}{p(s)/P^0} = \frac{1}{\tau_1 s}\left[1 - \left(\cosh\sqrt{\tau_2 s} + \frac{R_3}{R_2}\sqrt{\tau_2 s}\sinh\sqrt{\tau_2 s}\right)\left(\frac{\psi(s)/\Psi^0}{p(s)/P^0}\right)\right]\Bigg/\left(\frac{1}{3}+\frac{R_2}{R_1}+\frac{R_3}{R_1}\right) .$$

For cylinders

$$\frac{\psi(s)/\Psi^0}{p(s)/P^0} = \frac{2 r_2 k_2}{r_1^2}\sqrt{\frac{\alpha_2}{\alpha_1}}\; I_1^{11}(K_1^{22} I_0^{22} + K_0^{22} I_1^{22})\Big[k_2\sqrt{\alpha_2 s}\, I_0^{11}$$

$$\times\left(K_1^{21}\left\{I_0^{22} + R_3 k_2\sqrt{\alpha_2 s}\, I_1^{22}\right\} + I_1^{21}\left\{K_0^{22} - R_3 k_2\sqrt{\alpha_2 s}\, K_1^{22}\right\}\right)$$

$$+ k_1\sqrt{\alpha_1 s}\, I_1^{11}\times\left(K_0^{21}\left\{I_0^{22} + R_3 k_2\sqrt{\alpha_2 s}\, I_1^{22}\right\}\right.$$

$$\left. - I_0^{21}\left\{K_0^{22} - R_3 k_2\sqrt{\alpha_2 s}\, K_1^{22}\right\}\right)\Big]^{-1} ,$$

where for the fuel and clad of outer radii r_1 and r_2 respectively:

$$\alpha_1 = c_1/k_1$$

$$\alpha_2 = c_2/k_2 .$$

The superscript, mn, on a Bessel function denotes the argument, $\sqrt{\alpha_m s}\, r_n$. Also

$$\frac{\theta(s)/\Theta^0}{p(s)/P^0} = \frac{2 r_2}{r_1^2 k_1 \alpha_1 s\left[R_3 + \frac{r_2}{4k_1} + \frac{r_2}{k_2}\ln\frac{r_2}{r_1}\right]}$$

$$\left[1 - \frac{r_1(I_1^{21}[K_0^{22} - R_3 k_2\sqrt{\alpha_2 s}\, K_1^{22}] + K_1^{22}[I_0^{22} + R_3 k_2\sqrt{\alpha_2 s}\, I_1^{22}])}{r_2(K_1^{22} I_0^{22} + K_0^{22} I_1^{22})}\left(\frac{\psi(s)/\Psi^0}{p(s)/P^0}\right)\right] .$$

Equations 25, 26, 29, and 30 of Section IV - C are recognized as Taylor expansions of these expressions used to define single local time constants.

For the transfer function relating the voids of a channel to its power, the derivation of equation 37 of Section IV - C can be done more generally: The three functions, $\psi(z,t) = \psi_{avg}(t)\ \phi(z)$, $u(z)$, and $F(z)$ need not be constant with height. $F(z)$ is the reactivity importance function of the voids normalized, $\int_0^Z F(z)dz = Z$, and utilized to give $v(s) = \int_{X_0}^{Z} F(z)\ a(s)\ dz$. $\psi_{avg}(t)$ is the channel's surface power, and $\phi(z)$ its distribution normalized, $\int_0^Z \phi(z)d\,z = Z$. Solving the reformulated equations with ψ and u position dependent is straightforward. Use is made of

$$y(s) = \frac{e^{-sT(z)}}{u} \int^{z} f(z')\ \ e^{sT(z')}\ dz'$$

being the solution of

$$-\frac{\partial(uy)}{\partial z} + f(z) = \frac{\partial y}{\partial t} \quad .$$

The auxiliary function used is

$$T(z) = \int_0^z \frac{dz}{u(z)} \quad .$$

The results are

$$\frac{v_b(s)}{\psi_{avg_b}(s)} = \frac{1}{\rho\ell} \int_{X^0}^{Z} \frac{F(z)}{u(z)} \int_{X^0}^{z} \phi(z') \exp\left(s[T(z') - T(z)]\right) dz'\, dz$$

$$\frac{v_w(s)}{\psi_{avg\ w}(s)} = \frac{1}{\rho\ell} \int_{X^0}^{Z} \frac{F(z)}{u(z)} \exp\left(s\,[T(X^0) - T(z))dz \int_0^{X^0} \phi(z') \exp\right.$$

$$\left.\left(\frac{s}{w}\ [z' - X^0]\right)\right) dz' \quad .$$

Transfer functions stemming from pressure and feedwater variations have been treated by Beckjord, and need not be treated here. (His results for these two effects can be improved, however by proper spatial averaging.) It is worth pointing out that previous analytical treatments of void feedbacks have not separated the effect into the two parts as here, i.e. voids from power in the boiling region and from power in the non-boiling region.

Figure 22 is a block diagram of the transfer functions just treated. This is probably an adequate representation for most boiling reactors, although the effects of sections IV - E and IV - F are omitted due to a current lack of satisfactory theory. (Water acceleration effects have been investigated[21] to some extent. Evaluation of current formulae have not led to appreciable effects for typical EBWR conditions.) Figure 23 shows how feedbacks from the various reactor channels add.

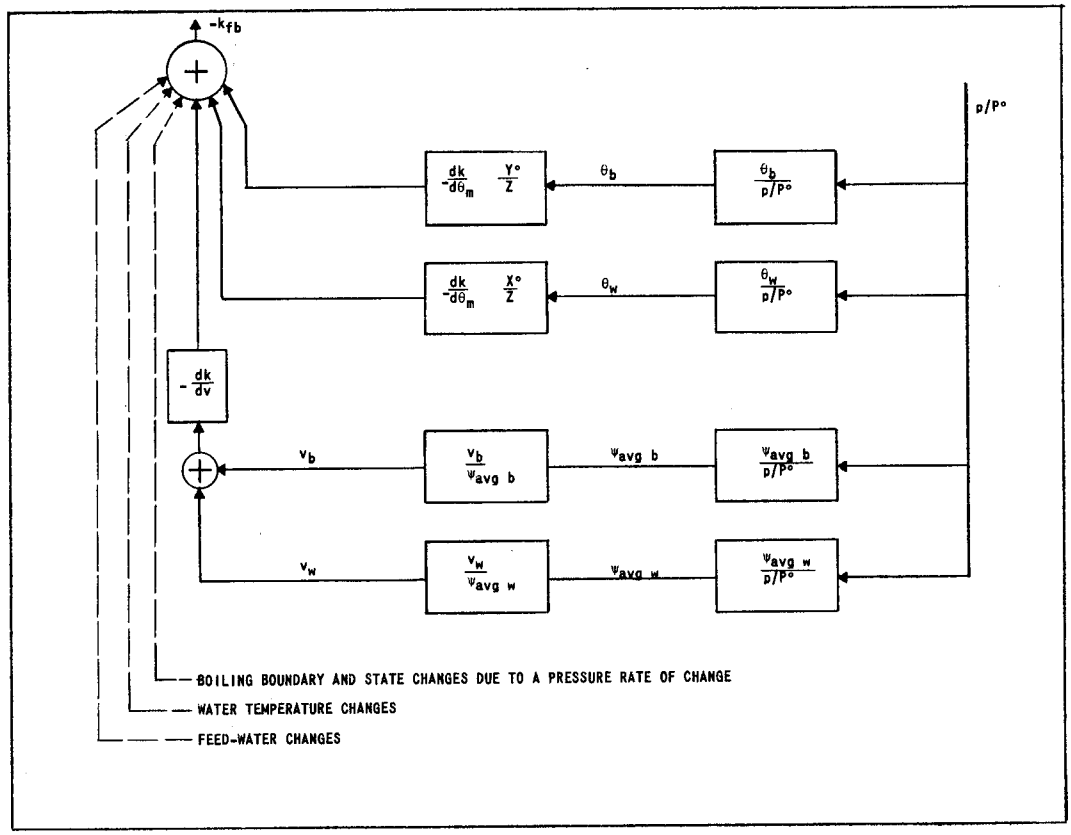

Fig. 22. The Combining of Feedback Transfer Functions in One Channel.

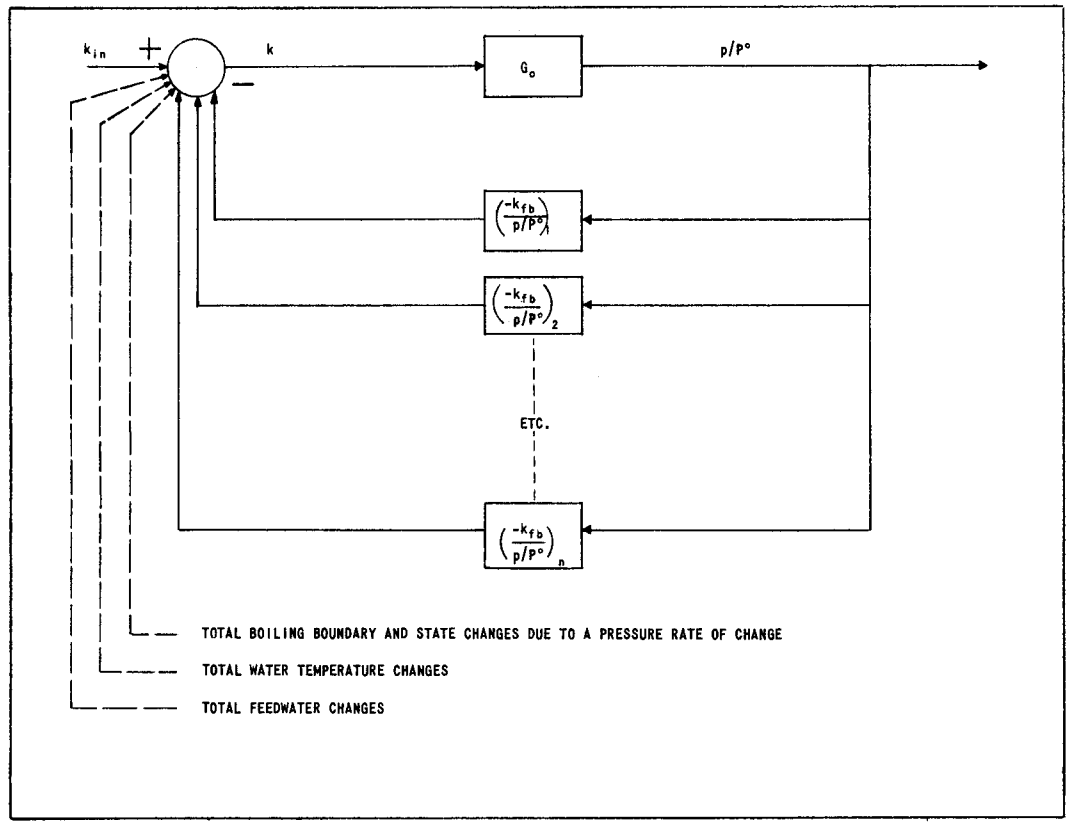

Fig. 23. The Combining of Feedbacks from Many Channels to give a Reactor Transfer Function.